Lawrence Berkeley Laboratory
UNIVERSITY OF CALIFORNIA

ENERGY & ENVIRONMENT
DIVISION

Submitted to Solar Energy Journal

DETAILED LOOP MODEL (DLM) ANALYSIS OF LIQUID SOLAR THERMOSIPHONS WITH HEAT EXCHANGERS

A. Mertol, W. Place, T. Webster, and R. Greif

June 1981

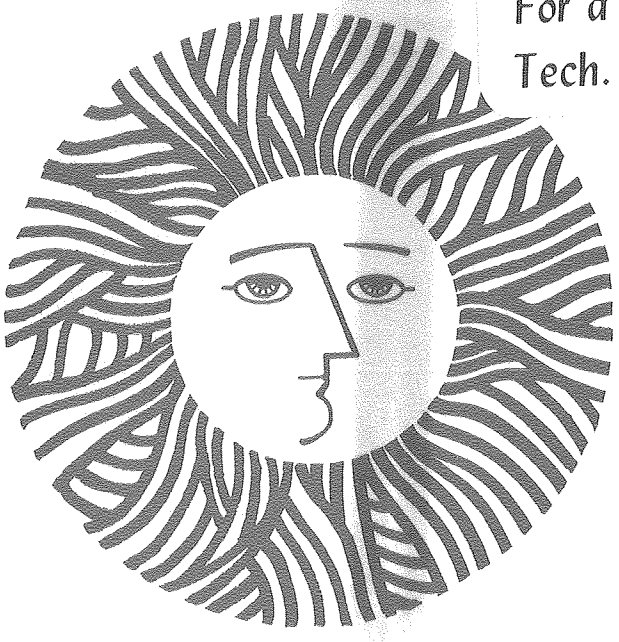

Prepared for the U.S. Department of Energy under Contract W-7405-ENG-48

DISCLAIMER

LBL-10699 Rev.
JUNE 1981

DETAILED LOOP MODEL (DLM) ANALYSIS OF LIQUID SOLAR THERMOSIPHONS WITH HEAT EXCHANGERS*

A. Mertol, W. Place and T. Webster

Passive Analysis and Design Group
Lawrence Berkeley Laboratory
University of California
Berkeley, California 94720 U.S.A.

and

R. Greif

Department of Mechanical Engineering
University of California
Berkeley, California 94720 U.S.A.

ABSTRACT

An analytical Detailed Loop Model (DLM) has been developed to analyze the performance of solar thermosiphon water heaters with heat exchangers in storage tanks. The model has been used to study the performance of thermosiphons as a function of heat exchanger characteristics, heat transfer fluids, flow resistances, tank stratification, and tank elevation relative to the collector. The results indicate that good performance can be attained with these systems compared to thermosiphons without heat exchangers.

---

*This work has been supported by the Research and Development Branch, Passive and Hybrid Division, of the Office of Solar Applications for Buildings, U.S. Department of Energy, under Contract No. W-7405-ENG-48.

1. INTRODUCTION

A common configuration for solar water heating systems is indicated in the following diagram:

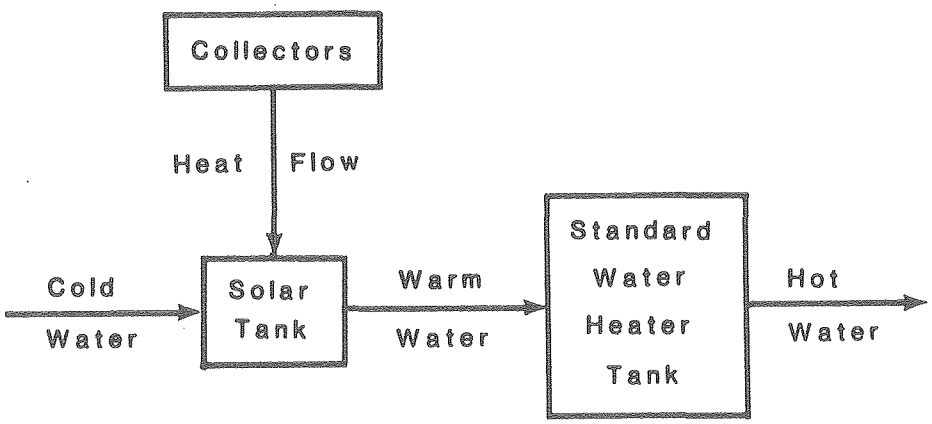

Heat flow from low-mass collectors to the solar preheat tank is customarily accomplished through a heat transfer fluid circulated by a small pump. The pump and controls represent an investment in terms of initial cost, maintenance and electrical operating costs. Heat flow from the collector absorber plate to the preheat storage tank can also be accomplished by natural convection. In the compact water heater, the absorber plate is part of the preheat storage tank housing, that is, the collector and tank are combined, and heat conducted through the plate is distributed through the water mass by natural convection. During periods of low solar radiation, reversed convection currents will carry energy back to the cooler absorber plate and substantial amounts of energy can be lost through the glazing, if movable insulation is not used. A variation of the compact heater, the "bread box heater," substitutes a series of cylindrical tanks for the single rectangular tank. This solves the structural problem of resisting the water pressure, but increases the convective and radiative losses due to the increase in the surface area. Another convective solar water heater is the thermosiphon, which uses a separate low-mass collector set below the storage tank.

Numerous studies of active heaters, compact heaters, and thermosiphons have been carried out (e.g., [1-45, 55]). A few of these studies have involved theoretical or experimental comparisons of systems [1-8]. Chauhan and Kadambi [1] tested a compact heater under two modes of operation. In one mode, natural convection was used to distribute absorbed energy into the bulk of the water. In the other mode, a propeller was used to increase the circulation rate of the water. Use of the propeller produced no appreciable enhancement of the system thermal performance, showing that natural convection alone is an adequate mode of heat transfer for this

configuration.

Place, Daneshyar and Kammerud [2] developed a simplified analysis to compare the average monthly predicted performance of a compact heater and a thermosiphon heater under the assumption of no nighttime reverse flow in the thermosiphon. That analysis predicted that the performance of the thermosiphon system would be substantially superior to that of the compact heater if movable insulation were not used to reduce nighttime losses from the compact heater. Bergquam, Young, Perry and Baughn [3] have drawn a similar conclusion based on experimental comparison of a bread box heater and a thermosiphon. In the same study, experimental comparisons were also made between a thermosiphon and several active solar heater configurations. The collection efficiency of the thermosiphon was found to be comparable to the best of the active systems; furthermore, accounting for the pump power makes apparent the superior overall system efficiency of the thermosiphon. These conclusions are substantiated by side-by-side tests of a thermosiphon and five active systems conducted by Fanney and Liu [7,8]. They found the system efficiencies of the active heaters to be 5 to 45% lower than the thermosiphon. Furthermore, if parasitic energy consumption were considered as energy required at a fossil-fueled electric generating plant, the effective system efficiencies of the active heaters were calculated to be 30 to 90% lower than the thermosiphon. The seeds of this conclusion can also be found in a much earlier work by Close [9]. His thermosiphon experiment indicated that during collection hours the average collector temperature was only slightly higher than the average storage tank temperature. Place, Daneshyar and Kammerud [2] argued that under these conditions, using a pump to increase the flow through the collector would have negligible effect on collection efficiency and could reduce system thermal performance by reducing the stratification.

These analytic and experimental studies have established the technical viability of using natural convection to transfer heat from the absorber plate to the storage mass if nighttime reverse flow can be suppressed. Furthermore, the widespread use of thermosiphons outside the United States is evidence of the market potential of these systems. However, thermosiphon heaters possess several features which continue to limit their application in the United States:

(1) Shielding the storage tank from view is often impractical;

(2) Mounting the tank above the collector creates structural problems; and

(3) Freezing of the low-mass collector is a serious hazard in almost all United States climates.

The first problem is an aesthetic issue which can be addressed in a number of ways; however, in those cases where shielding the storage tank from view is impractical, many consumers will be prompted to choose an active heater or do without solar water heating. The structural problems are not severe in new construction, but they will limit some retrofit applications of thermosiphon heaters. By far the most critical concern at this point in time is the development of reliable, cost-effective freeze protection for thermosiphon heaters. A number of possibilities exist, among which are:

(1) Use of valves to isolate the tank and drain the collectors when freezing is imminent [5-8];

(2) Use of a freeze-resistant plastic collector [10,11]; and

(3) Use of a non-freezing collection fluid which transfers heat to the storage water through a heat exchanger in the storage tank, such as shown in Fig. 1(a).

All of the approaches listed above have disadvantages. For convenience, a drain-down system would probably use thermostatic valves or electrically activated solenoid valves. Thermostatic valves present problems in design and reliability. Studies on systems which use solenoid valves [5-8] indicate that in addition to increasing the initial cost and adding complexity (in terms of the valves as well as the controls hardware), they are prone to failure. The durability of highly flexible, freeze-resistant plastic collectors subjected to mains pressure, temperature cycling and ultraviolet radiation has not been adequately assessed; also, the low thermal conductivity of the material can limit collection efficiency [10,11]. Using a non-freezing heat transfer fluid with a heat exchanger also adds complexity and reduces system performance as a result of the non-ideal heat-transfer associated with any practical heat exchanger design. Thermosiphon heat transfer fluids can be used in a single-phase mode (liquid throughout) or in a two-phase mode (some liquid and some vapor). Propylene glycol (p-glycol) would be appropriate to the former mode; some freons would be appropriate to the latter mode [12-16]. The work presented in this paper is an initial effort to quantify the behavior of thermosiphons with heat exchangers; p-glycol was chosen as the heat transfer fluid in the initial studies because of its low toxicity and familiarity to the solar industry. Recent trends indicate that p-glycol will be accepted for use with single-wall heat exchangers [17]. In addition to addressing freeze-protection issues, the current work assesses the performance implications of various system parameters. As already indicated, previous studies [2,3,5-9] have established that good thermal performance can be achieved by specific system configurations under certain conditions of operation, but none of the studies has examined system performance over an adequate range of parameters. In addition to the aforementioned studies, a number of

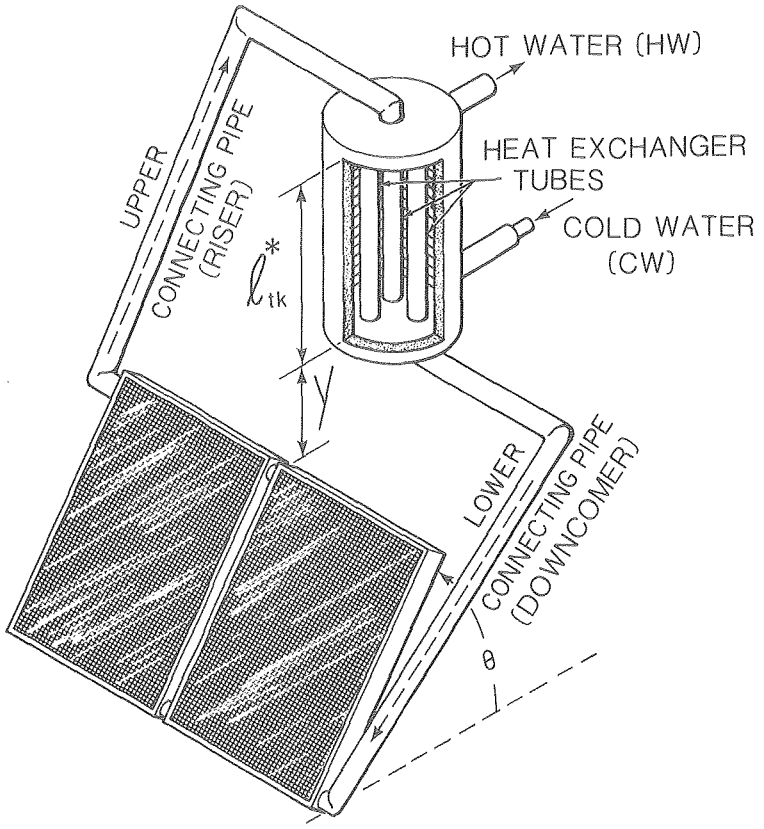

FIG. 1(a)

XBL 803-6909B

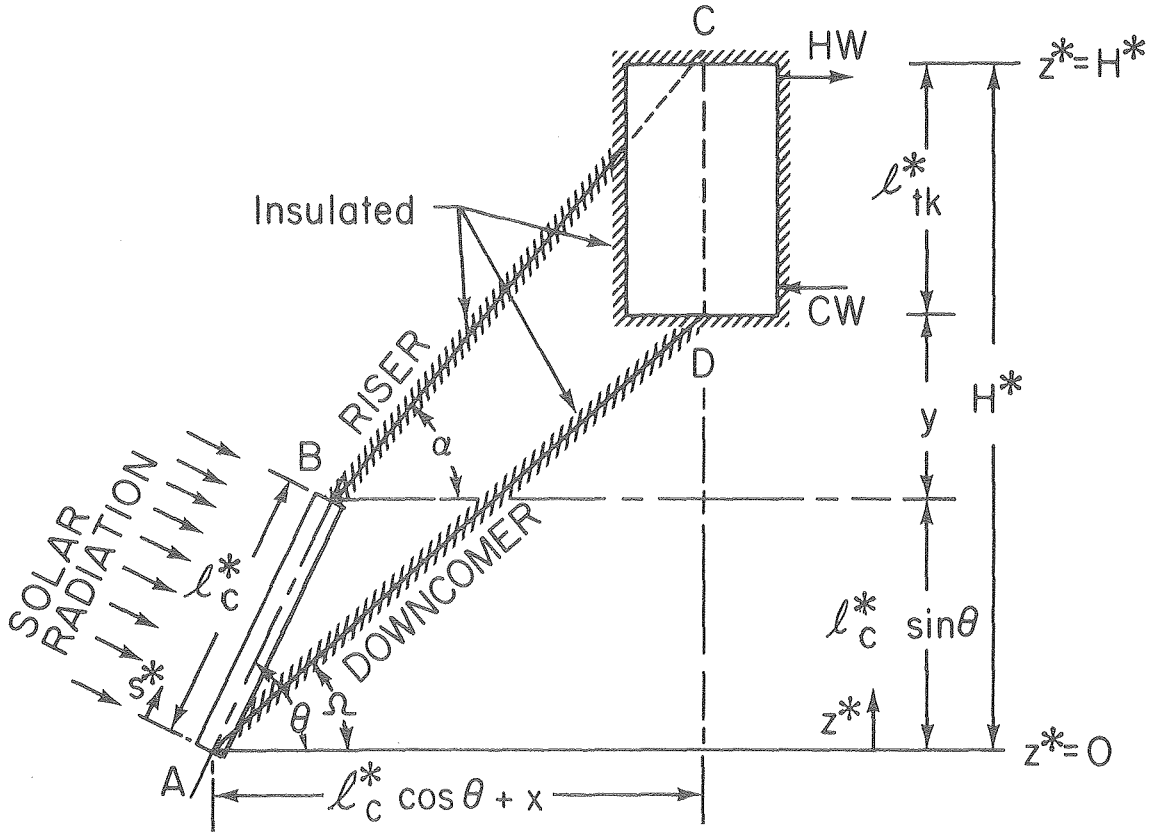

FIG. 1(b)

XBL806-7155A

other thermosiphon publications are summarized in the Appendix.

2. ANALYSIS

The following analysis enables prediction of the transient and steady-state behavior of a thermosiphon solar water heater with a heat exchanger in the storage tank. The system consists of bulk storage water in a tank and a heat transfer fluid circulating in a closed loop consisting of a flat-plate solar collector, insulated connecting pipes (riser and downcomer) and a heat exchanger inside the tank (cf. Figs. 1(a) and 1(b)).

2.1 Heat Transfer Fluid

To utilize a heat exchanger in a storage tank entails some compromise in the system performance. The effect of the heat exchanger can be mitigated if a single wall heat exchanger is used. Single wall heat exchangers have been the subject of considerable controversy in the solar industry, but recent trends indicate that they are finally being considered for use when special provisions are met [17]. One of these provisions is that the collection fluid (heat transfer fluid) must be "practically non-toxic"; i.e., it must have a Gosselin toxicity rating of 1, which means the likely lethal dose for a human being is greater than 15 gm/kg body weight. In addition to being non-toxic the fluid must be chemically stable over the operating range of the system and also be non-freezing at very low ambient temperatures. While p-glycol meets the toxicity and anti-freeze requirements [41], there is some concern regarding its chemical stability, because of its tendency to decompose into acids when exposed to high temperatures and oxygen. However, some recent industry tests indicate that p-glycol containing the proper inhibitors can operate at temperatures up to 175^{o}C (350^{o}F) for extended periods without significant degradation [57,58]. Also, when compared to pumped systems, temperatures in thermosiphon systems are less likely to reach collector stagnation temperature because of losses from the tank and the piping. Extreme temperatures could also be avoided by using a temperature relief valve set below any safety valve settings.

The toxicity hazard of p-glycol in this application may be minimized because solar systems contain a limited amount of the collector fluid that would most likely be diluted before consumption. A simple calculation assuming 0.0075 m^3 (2 gal) of p-glycol and 0.15 m^3 (40 gal) storage tank shows that homogeneous dilution in the storage tank of all of the collector fluid will produce a dose of less than 1 gm/kg body weight for a child consuming a glass of water--well below the lethal dose of fluids with a toxicity rating

of 1. It thus appears that there is an ample margin of safety for using p-glycol for solar applications with a single wall heat exchanger [17]. Even with these assurances, further research still needs to be done and the following protective measures should be considered as a minimum:

(1) Using a non-toxic dye in the heat transfer fluid;

(2) Providing extensive warning stickers specifying the type of fluid and what to do in case of a leak, etc.;

(3) Using a copper-wall heat exchanger; and

(4) Designing the system so that the maximum loop pressure will never exceed normal city water pressure inside the storage tank [17].

For the studies reported in this paper, a propylene-glycol solution, 60% by weight, was selected as the heat transfer fluid. The properties of p-glycol and water are shown in Fig. 2.

2.2 Basic Assumptions

The basic conservation equations--the continuity, momentum and energy equations--are averaged over the cross-section normal to the flow direction so that the only space coordinate, s*, varies along the thermosiphon loop. The flow is assumed to be laminar and the density of the circulating fluid is taken to be constant, except in the buoyancy producing term of the momentum equation, where it is assumed to vary linearly with temperature (Boussinesq approximation). The viscosity of the circulating fluid is evaluated at the average temperature of each system component in accordance with the temperature dependence shown in Fig. 2. Simulating the convection effects necessary to determine spatial temperature variations in a tank containing a heat exchanger can be a complicated and expensive analytic procedure. In order to simplify the thermal model, a linear temperature variation is assumed along the vertical axis of the tank. The temperature differential from top to bottom of the tank is one of the inputs to the computer simulation. In order to test the sensitivity of system performance to tank stratification, several simulations were performed based on assumed temperature differentials ranging from zero up to $11^{o}C$. The results of those simulations are presented and discussed in section 4.1. The average temperature of the storage water is determined at each computational time step by performing an energy balance on the tank. Other simplifying assumptions include the following:

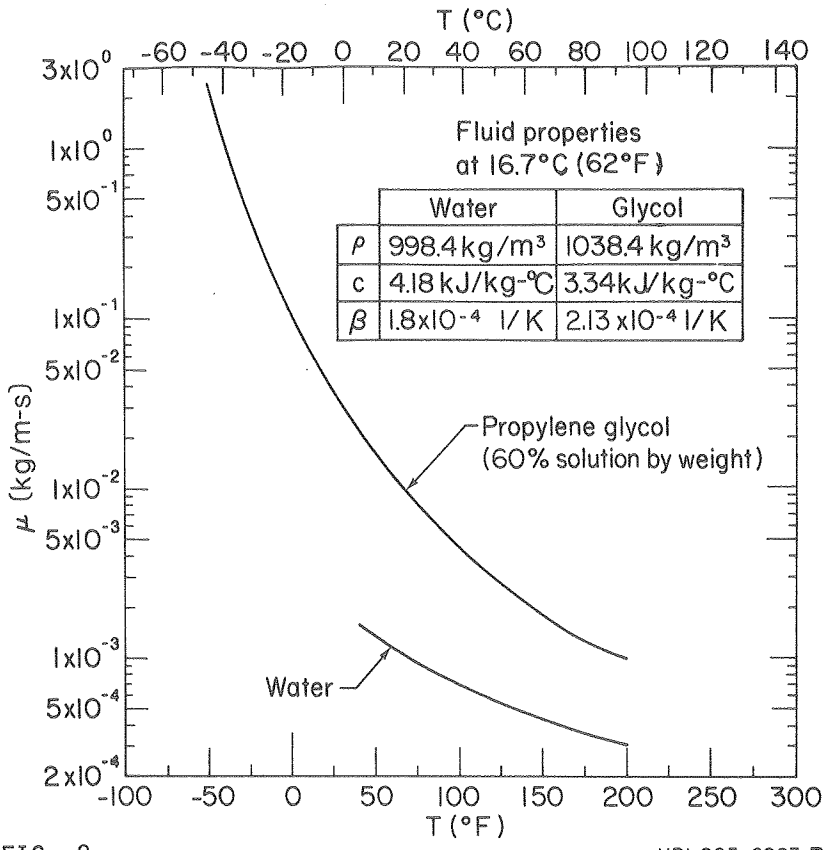

FIG. 2

XBL805-6993 B

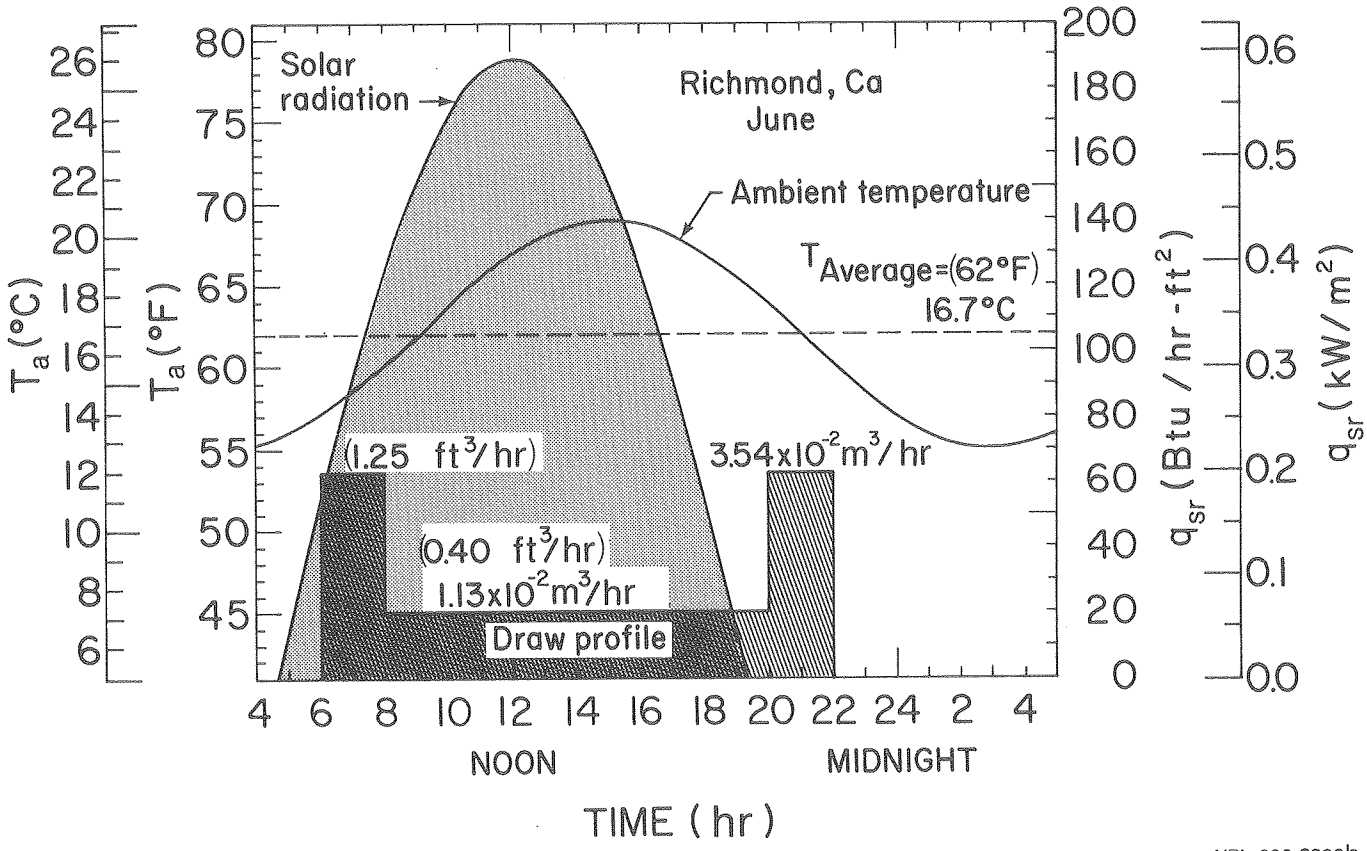

FIG. 3

XBL 803-6908b

(1) Negligible collector heat capacity;

(2) Collector parameters based on actual data for a typical one-cover, selective surface collector;

(3) Constant overall heat transfer coefficients for the collector and heat exchanger (U_L and U_{he});

(4) Sine function approximations for the solar radiation on the absorber cover plate and the ambient air temperature based on monthly average data [54] (cf. Fig. 3); and

(5) A total daily draw of 0.278 m^3 (73 gal) (cf. Fig. 3).

The system dimensions and the important parameters used in the analysis are presented in Table 1, and unless otherwise specified, pertain to all results.

2.3 Mathematical Model

From the equation of continuity for one-dimensional incompressible flow, $D\rho/Dt = 0$ so that the volumetric flow rate or the velocity in each component of the system (i.e., collector tubes, headers, connecting pipes, and heat exchanger tubes) is only a function of time:

$$Q(t) = \frac{\pi d^{*2}}{4} v(t) \tag{1}$$

The momentum equation for the entire thermosiphon loop is obtained by piecewise integration over each part of the loop which yields:

$$\frac{\ell_c^*}{A_c}\frac{dQ_c}{dt} + \frac{\ell_h^*}{A_h}\frac{dQ_h}{dt} + \frac{\ell_{cp}^*}{A_{cp}}\frac{dQ_{cp}}{dt} + \frac{\ell_{he}^*}{A_{he}}\frac{dQ_{he}}{dt} = -\frac{1}{\rho_0}\oint dp$$

$$- g\oint\left[1 - \beta(T - T_0)\right]dz^* - \left(f_c\frac{\ell_c^*}{d_c^*} + K_c\right)\frac{Q_c^2}{2A_c^2}$$

$$- \left(f_h\frac{\ell_h^*}{d_h^*}B + K_hB'\right)\frac{Q_h^2}{2A_h^2} - \left(f_{cp}\frac{\ell_{cp}^*}{d_{cp}^*} + K_{cp}\right)\frac{Q_{cp}^2}{2A_{cp}^2} - \left(f_{he}\frac{\ell_{he}^*}{d_{he}^*} + K_{he}\right)\frac{Q_{he}^2}{2A_{he}^2} \tag{2}$$

TABLE 1. SYSTEM DIMENSIONS AND PARAMETERS

A_{cc} = 2 x 1.95 m^2 (2 x 21 ft^2)	N = 2 x 9
d^*_c = 0.95 cm (0.38 in)	S_t = 20080 kJ/m^2-day (1766 Btu/ft^2-day)
d^*_{cp} = 2.60 cm (1.03 in)	T_s = 16.7°C (62°F)
d^*_h = 2.68 cm (1.06 in)	ΔT = 5.5°C (10°F)
d^*_{he} = 5.04 cm (1.98 in)	$U_c = F'U_L$ = 4.201 W/m^2-°C (0.741 Btu/hr-ft^2-°F)
d^*_{tk} = 50.8 cm (20 in)	U_{he} = 170 W/m^2-°C (30 Btu/hr-ft^2-°F)
F' = 0.9	U_{in} = 0.85 W/m^2-°C (0.15 Btu/hr-ft^2-°F)
ℓ^*_c = 1.75 m (5.75 ft)	V = 0.302 m^3 (80 gal)
ℓ^*_h = 4 x 1.12 m (4 x 3.67 ft)	$\dot{V}$ = 0.278 m^3/day (73 gal/day)
ℓ^*_{he} = 1.52 m (5 ft)	θ = 45
ℓ^*_{cp} = 4.54 m (14.9 ft)	$\tau\alpha$ = 0.86
ℓ^*_{tk} = 1.52 m (5 ft)	No. of elbows = 10
M = 3	No. of tees = 4

Circulating Fluid: Propylene-Glycol (60% by weight)

CLIMATE: See Figure 3

Note that $-\rho_o^{-1} \oint dp$ reduces to zero.

The friction coefficient for laminar flow can be expressed in terms of the Reynolds number by $f = 64/Re$, where $Re = 4\rho Q/d^*$. Then the loss coefficient, K, can be expressed in terms of the friction coefficient by $K = f(\ell/d)_{eq}$. Note that the friction and the friction loss coefficient vary for each system component.

Equation (2) is re-written in terms of the volumetric flow rate inside the connecting pipes, Q_{cp}, by using the conservation of mass relation:

$$\rho_o Q_{cp} = \rho_o M Q_{he} = \rho_o N Q_c = \rho_o Q_h$$

where M and N are the total number of heat exchanger and collector tubes, respectively.

Substituting flow rates from Eq. (3) into Eq. (2) and simplifying yields:

$$\frac{dQ_{cp}}{dt} = \frac{\beta g A_{cp}}{\ell^*_{cp} L_s} \oint (T - T_o) dz^* - \frac{8\pi d^*_{cp} \mu_o}{\ell^*_{cp} A_{cp} \rho_o L_s} \left(f_e \frac{\ell^*_{cp}}{d^*_{cp}} + K_e \right) Q_{cp} \qquad (4)$$

where

$$L_s = 1 + \left(\frac{\ell^*_h}{\ell^*_{cp}}\right)\left(\frac{d^*_{cp}}{d^*_h}\right)^2 + \frac{1}{N}\left(\frac{\ell^*_c}{\ell^*_{cp}}\right)\left(\frac{d^*_{cp}}{d^*_c}\right)^2 + \frac{1}{M}\left(\frac{\ell^*_{he}}{\ell^*_{cp}}\right)\left(\frac{d^*_{cp}}{d^*_{he}}\right)^2 \qquad (5a)$$

$$f_e = \frac{\mu_{cp}}{\mu_o} + B\left(\frac{\mu_h}{\mu_o}\right)\left(\frac{\ell^*_h}{\ell^*_{cp}}\right)\left(\frac{d^*_{cp}}{d^*_h}\right)^4 + \frac{1}{N}\left(\frac{\mu_c}{\mu_o}\right)\left(\frac{\ell^*_c}{\ell^*_{cp}}\right)\left(\frac{d^*_{cp}}{d^*_c}\right)^4$$

$$+ \frac{1}{M}\left(\frac{\mu_{he}}{\mu_o}\right)\left(\frac{\ell^*_{he}}{\ell^*_{cp}}\right)\left(\frac{d^*_{cp}}{d^*_{he}}\right)^4 \qquad (5b)$$

and

$$K_e = \frac{\mu_{cp}}{\mu_o} \sum\left(\frac{\ell}{d}\right)_{eq_{cp}} + B'\left(\frac{\mu_h}{\mu_o}\right)\left(\frac{d^*_{cp}}{d^*_h}\right)^3 \sum\left(\frac{\ell}{d}\right)_{eq_h}$$

$$+ \frac{1}{N}\left(\frac{\mu_c}{\mu_o}\right)\left(\frac{d^*_{cp}}{d^*_c}\right)^3 \sum\left(\frac{\ell}{d}\right)_{eq_c} + \frac{1}{M}\left(\frac{\mu_{he}}{\mu_o}\right)\left(\frac{d^*_{cp}}{d^*_{he}}\right)^3 \sum\left(\frac{\ell}{d}\right)_{eq_{he}} \qquad (5c)$$

B and B' in Eqs. 5(b) and 5(c) are the header loss modifiers to account for effects of tube to header junctions which are given by:

$$B = \frac{2}{N^2} \sum_{i=1}^{N} (N - i + 1) \quad \text{and} \quad B' = \frac{2}{N^2} \sum_{i=1}^{N} (N - i + 1)^2 \tag{5d}$$

To solve for the volumetric flow rate from Eq. (4), it is necessary to obtain the temperature variation, $T(s^*,t)$. The energy equations for the system components are given as follows:

(i) Collector tubes:

$$\frac{\partial T}{\partial t} + \frac{Q_c}{A_c} \frac{\partial T}{\partial s^*} = \frac{4}{\rho_o c_o d_c^*} q_c (s^*,t) \tag{6}$$

where

$$q_c (s^*,t) = \frac{A_{cc}}{\pi d_c^* \ell_c^* N} \left\{ F' \tau\alpha q_{sr}(t) - F' U_L [T(s^*,t) - T_a(t)] \right\} \tag{7}$$

The following "sine" function approximations are used for the solar radiation on the absorber cover plate, $q_{sr}(t)$, and the ambient air temperature, $T_a(t)$ (cf. Fig.3):

$$q_{sr}(t) = q_{max} \sin (\pi t/P^*) \tag{8}$$

where

$$q_{max} = \frac{\pi}{2} \frac{S_t}{P^*} \tag{9}$$

and

$$T_a(t) = T_{ave} + T_{amp} \sin [2\pi(t - 9)/24] \tag{10}$$

Note that S_t and P^* are the total daily solar radiation [54] and the duration of sunshine (time between sunrise and sunset), respectively.

(ii) Connecting pipes (riser and downcomer):

$$\frac{\partial T}{\partial t} + \frac{Q_{cp}}{A_{cp}} \frac{\partial T}{\partial s^*} = - \frac{4U_{in}}{\rho_o c_o d_{cp}^*} \left[T(s^*,t) - T_a(t) \right] \tag{11}$$

The R.H.S. of Eq. (11) corresponds to the energy loss through the insulation.

(iii) Heat exchanger tubes:

$$\frac{\partial T}{\partial t} + \frac{Q_{he}}{A_{he}} \frac{\partial T}{\partial s^*} = - \frac{4U_{he}}{\rho_o c_o d^*_{he}} \left[T(s^*,t) - T_{tk}\ (s^*,t)\right] \tag{12}$$

The storage water temperature inside the tank, T_{tk}, is assumed to vary linearly with vertical position, z*. The temperature variation is given by:

$$T_{tk}(z^*,t) = T_s \left\{h(t) + \frac{\Delta T}{T_s \ell^*_{tk}} \left[z^* - (H^* - \ell^*_{tk})\right]\right\} \tag{13}$$

A range of temperature differences (ΔT) between the top and bottom of the tank is assumed. The unknown function h(t) in Eq. (13) must be determined from the energy balance on the storage tank.

(iv) Storage tank: The energy balance on the storage tank which includes energy transfer through the heat exchanger walls, losses through the storage tank insulation, energy delivery to the draw and the storage term is given as follows:

$$\rho_w c_w \frac{\pi d^{*2}_{mt}}{4} \ell^*_{tk} \frac{d}{dt} \left[\frac{1}{\ell^*_{tk}} \int_{H^*-\ell^*_{tk}}^{H^*} T_{tk}(z^*,t)\, dz^*\right]$$

$$= \pi d^*_{he} \ell^*_{tk} MU_{he} \left\{\frac{1}{\ell^*_{tk}} \int_{H^*-\ell^*_{tk}}^{H^*} [T(z^*,t) - T_{tk}(z^*,t)]\, dz^*\right\}$$

$$- \pi d^*_{tk} \ell^*_{tk} U_{in} \left[\frac{1}{\ell^*_{tk}} \int_{H^*-\ell^*_{tk}}^{H^*} T_{tk}(z^*,t)\, dz^* - T_a(t)\right]$$

$$- \rho_w \dot{V} c_w \left[T_{max}(t) - T_s\right] \tag{14}$$

where

$$T_{max}(t) = T_{tk}(H^*,t) = T_s\left[h(t) + \frac{\Delta T}{T_s}\right] \tag{15a}$$

and

$$d^*_{mt} = (d^{*2}_{tk} - Md^{*2}_{he})^{1/2} \tag{15b}$$

Note that the exit temperature of the draw is assumed to be the maximum temperature inside the storage tank which is given by Eq. (15a). The draw profile as a function of time is plotted in Fig. 3.

The equations of the system, (4), (6), (11), (12), and (14), are made dimensionless by the following substitutions:

$$\phi \equiv \frac{T - T_o}{q_{max}/U_c} \equiv \frac{T - T_s}{q_{max}/U_c}, \quad w_i \equiv \frac{Q_i}{Q_{ch}}, \quad \tau \equiv \frac{t}{L_T/V}$$

$$P \equiv \frac{P^*}{L_T/V}, \quad s,z,H \equiv \frac{s^*,z^*,H^*}{L_T}, \text{ respectively}, \quad d_i \equiv \frac{d^*_i}{d^*_{cp}}$$

and

$$\ell_i \equiv \frac{\ell^*_i}{L_T} \tag{16a}$$

where

$$i = c, cp, h, he, tk, \text{ respectively}$$

and

$$L_T \equiv \ell^*_c + \ell^*_{cp} + \ell^*_{he} \tag{16b}$$

The characteristic volumetric flow rate, Q_{ch}, which is defined as the product of the cross-sectional area of the connecting pipe, A_{cp}, and the characteristic velocity, V, is given by:

$$Q_{ch} = A_{cp}V = \frac{\pi d^{*2}_{cp}}{4}\left(\frac{g\beta L_T d^*_{cp} q_{max}}{4c_o\mu_o}\right)^{1/2} \tag{17}$$

The dimensionless system parameters are given as follows:

(1) Thermosiphon convection parameter:

$$\Gamma = 4 \frac{Gr_m}{Re_{ch}^2} \left(\frac{L_T}{d^*_{cp}} \right)^2 = 4\ Ri \left(\frac{L_T}{d^*_{cp}} \right)^2 \tag{18a}$$

(2) Collector heat transfer parameter: $$D_c = \frac{4U_c L_T}{\rho_o c_o d^*_{cp} V} \tag{18b}$$

(3) Heat exchanger heat transfer parameter: $$D_{he} = \frac{4U_{he} L_T}{\rho_o c_o d^*_{cp} V} \tag{18c}$$

(4) Insulation loss parameter: $$D_{in} = \frac{4U_{in} L_T}{\rho_o c_o d^*_{cp} V} \tag{18d}$$

(5) Fluid parameter: $$\delta = \frac{\rho_o}{\rho_w} \frac{c_o}{c_w} \tag{18e}$$

(6) Solar radiation parameter: $$\psi = \frac{q_{max}}{T_o U_c} \tag{18f}$$

(7) Draw parameter: $$\zeta(t) = \frac{\dot{4}VL_T}{\pi d^{*2}_{mt} \ell^*_{tk} V} \tag{18g}$$

(8) Collector geometry parameter: $$\xi = \frac{A_{cc} d^*_{cp}}{\pi \ell^*_c N d^{*2}_c} \tag{18h}$$

(9) Connecting pipe parameter: $$\gamma = d^*_{cp} / \ell^*_{cp} \tag{18i}$$

The modified thermosiphon Grashof, Reynolds and Richardson numbers based on the characteristic velocity, V, are defined as follows (cf. Creveling et al. [49]):

$$Gr_m = \frac{g\rho_o d^{*3}_{cp}\beta q_{max}}{\mu_o^2 c_o V} \tag{19a}$$

$$Re_{ch} = \frac{\rho_o V d^*_{cp}}{\mu_o} \tag{19b}$$

and

$$Ri = \frac{g d^*_{cp}\beta q_{max}}{\rho_o c_o V^3} = \frac{Gr_m}{Re^2_{ch}} \tag{19c}$$

The dimensionless forms of Eqs. (4), (6), (11), (12), and (14) then become:

(a) Momentum equation:

$$\frac{dw_{cp}}{d\tau} + 2\frac{\Gamma}{L_s}(f_e + K_e\gamma)w_{cp} = \frac{\Gamma}{D_c}\frac{1}{\ell_{cp}L_s}\oint \phi dz \tag{20}$$

(b) Energy equations:

(i) Collector tubes:

$$\frac{\partial\phi}{\partial\tau} + \left(\frac{1}{d_c}\right)^2 w_c \frac{\partial\phi}{\partial s} = D_c\xi\left[F'\tau\alpha \sin(\pi\tau/P) - (\phi - \phi_a)\right] \tag{21}$$

(ii) Connecting pipes:

$$\frac{\partial\phi}{\partial\tau} + w_{cp}\frac{\partial\phi}{\partial s} = -D_{in}(\phi - \phi_a) \tag{22}$$

(iii) Heat exchanger tubes:

$$\frac{\partial\phi}{\partial\tau} + \left(\frac{1}{d_{he}}\right)^2 w_{he}\frac{\partial\phi}{\partial s} = -\frac{D_{he}}{d_{he}}(\phi - \phi_{tk}) \tag{23}$$

and

(iv) Storage tank:

$$\frac{dh(\tau)}{d\tau} + \left[D_{he} M \frac{d_{he}}{d_{mt}^2} \delta + d_{tk} \frac{D_{in}}{d_{mt}^2} \delta + \zeta(\tau) \right] h(\tau)$$

$$= D_{he} M \frac{d_{he}}{d_{mt}^2} \delta \left[\frac{\psi}{\ell_{tk}} \int_{H-\ell_{tk}}^{H} \phi \, dz + \left(1 - \frac{\Delta T}{2T_s} \right) \right]$$

$$+ \frac{D_{in}}{d_{mt}^2} d_{tk} \delta \left[\psi \phi_a + \left(1 - \frac{\Delta T}{2T_s} \right) \right] + \zeta(\tau) \left(1 - \frac{\Delta T}{T_s} \right) \qquad (24)$$

3. METHOD OF SOLUTION

The governing equations of the system, Eqs. (20)-(24) have been solved numerically using a finite difference method to calculate the variations of the temperature and flow rates in each system component. The backward difference formula was used for the spatial derivatives and the forward difference formula was used for the time derivatives. The integrals in Eqs. (20) and (24) were evaluated by using the trapezoidal rule. The marching scheme was taken in the flow direction. Therefore two sets of governing equations were used to study both forward and reverse flow effects on the system. The only difference between the forward and reverse flow equations appeared in the buoyancy term in the momentum equation. The equations for forward flow are given by:

(a) Momentum equation:

$$\frac{w_{cp_{n+1}} - w_{cp_n}}{\Delta\tau} + 2 \frac{\Gamma}{L_s} (f_e + K_e \gamma) w_{cp_n} = \frac{\Gamma}{D_c} \frac{1}{\ell_{cp} L_s} \oint \phi_{i,n+1} dz \qquad (25)$$

where

$$\oint \phi_{i,n+1}\, dz = \underbrace{\left(\tfrac{1}{2}\phi_{J,n+1} + \sum_{i=1}^{K-1} \phi_{i,n+1} + \tfrac{1}{2}\phi_{K,n+1}\right) \Delta s_c \sin\theta}_{\text{collector}}$$

$$+ \underbrace{\left(\tfrac{1}{2}\phi_{K,n+1} + \sum_{i=1}^{I-1} \phi_{i,n+1} + \tfrac{1}{2}\phi_{I,n+1}\right) \Delta s_r \sin\alpha}_{\text{riser}}$$

$$- \underbrace{\left(\tfrac{1}{2}\phi_{I,n+1} + \sum_{i=1}^{S-1} \phi_{i,n+1} + \tfrac{1}{2}\phi_{S,n+1}\right) \Delta z}_{\text{ht.exchgr.}}$$

$$- \underbrace{\left(\tfrac{1}{2}\phi_{S,n+1} + \sum_{i=1}^{J-1} \phi_{i,n+1} + \tfrac{1}{2}\phi_{J,n+1}\right) \Delta s_d \sin\Omega}_{\text{downcomer}} \qquad (26)$$

Substituting Eq. (26) into Eq. (25) yields:

$$w_{cp_{n+1}} = w_{cp_n}\left[1 - 2\frac{\Gamma}{L_s}(f_e + K_e\gamma)\Delta\tau\right] + \frac{\Gamma}{D_c}\frac{\Delta\tau}{\ell_{cp} L_s}$$

$$\left[\left(\frac{1}{2}\phi_{J,n+1} + \sum_{i=1}^{K-1}\phi_{i,n+1} + \frac{1}{2}\phi_{K,n+1}\right)\Delta s_c \sin\theta\right.$$

$$+ \left(\frac{1}{2}\phi_{K,n+1} + \sum_{i=1}^{I-1}\phi_{i,n+1} + \frac{1}{2}\phi_{I,n+1}\right)\Delta s_r \sin\alpha$$

$$- \left(\frac{1}{2}\phi_{I,n+1} + \sum_{i=1}^{S-1}\phi_{i,n+1} + \frac{1}{2}\phi_{S,n+1}\right)\Delta z$$

$$\left. - \left(\frac{1}{2}\phi_{S,n+1} + \sum_{i=1}^{J-1}\phi_{i,n+1} + \frac{1}{2}\phi_{J,n+1}\right)\Delta s_d \sin\Omega\right] \qquad (27)$$

(b) Energy equations:

(i) Collector tubes:

$$\frac{\phi_{i,n+1} - \phi_{i,n}}{\Delta\tau} + \left(\frac{1}{d_c}\right)^2 w_{c_n} \frac{\phi_{i,n} - \phi_{i-1,n}}{\Delta s_c} =$$

$$D_c\xi\left\{F'\tau\alpha \sin\left[\pi/P\ (\tau + \Delta\tau)\right] - (\phi_{i,n+1} - \phi_{a_{n+1}})\right\} \qquad (28)$$

Combining the terms yields:

$$\phi_{i,n+1} = \left(\frac{1}{1 + D_c\xi\Delta\tau}\right)\left\{\phi_{i,n}\left(1 - \frac{w_{c_n}}{d_c^2}\frac{\Delta\tau}{\Delta s_c}\right) + \phi_{i-1,n} w_{c_n} \frac{\Delta\tau}{\Delta s_c}\left(\frac{1}{d_c^2}\right)\right.$$

$$\left. + D_c\xi\Delta\tau\left[F'\tau\alpha \sin\left[\pi/P\ (\tau + \Delta\tau)\right] + \phi_{a_{n+1}}\right]\right\} \qquad (29)$$

(ii) Connecting pipes:

$$\frac{\phi_{i,n+1} - \phi_{i,n}}{\Delta\tau} + w_{cp_n}\frac{\phi_{i,n} - \phi_{i-1,n}}{\Delta s_{r,d}} = -D_{in}\left(\phi_{i,n+1} - \phi_{a_{n+1}}\right) \qquad (30)$$

or

$$\phi_{i,n+1} = \left(\frac{1}{1 + D_{in}\Delta\tau}\right)\left[\phi_{i,n}\left(1 - w_{cp_n}\frac{\Delta\tau}{\Delta s_{r,d}}\right)\right.$$

$$\left. + \phi_{i-1,n} w_n \frac{\Delta\tau}{\Delta s_{r,d}} + D_{in}\phi_{a_{n+1}}\Delta\tau\right] \qquad (31)$$

(iii) Heat exchanger tubes:

$$\frac{\phi_{i,n+1} - \phi_{i,n}}{\Delta\tau} + \frac{w_{he_n}}{d_{he}^2} \frac{\phi_{i,n} - \phi_{i-1,n}}{\Delta z} = -\frac{D_{he}}{d_{he}} (\phi_{i,n+1} - \phi_{tk_{i,n+1}}) \tag{32}$$

or

$$\phi_{i,n+1} = \frac{1}{\left(1 + \frac{D_{he}}{d_{he}} \Delta\tau\right)} \left\{ \phi_{i,n} \left(1 - \frac{w_{he_n}}{d_{he}^2} \frac{\Delta\tau}{\Delta z}\right) + \phi_{i-1,n} \frac{w_{he_n}}{d_{he}^2} \frac{\Delta\tau}{\Delta z} + \phi_{tk_{i,n+1}} \frac{D_{he}}{d_{he}} \Delta\tau \right\} \tag{33}$$

and

iv) Storage tank:

$$\frac{h_{n+1} - h_n}{\Delta\tau} + \left[D_{he} M \frac{d_{he}}{d_{mt}^2} \delta + \frac{D_{in}}{d_{mt}^2} d_{tk} \delta + \zeta_{n+1} \right] h_{n+1}$$

$$= D_{he} M \frac{d_{he}}{d_{mt}^2} \delta \left\{ \frac{\psi}{\ell_{tk}} \left[\frac{1}{2} \phi_{I,n+1} + \sum_{i=1}^{S-1} \phi_{i,n+1} + \frac{1}{2} \phi_{S,n+1} \right] \Delta z + \left(1 - \frac{\Delta T}{2T_s}\right) \right\} + d_{tk} \frac{D_{in}}{d_{mt}^2} \delta \left[\psi \phi_{a_{n+1}} + \left(1 - \frac{\Delta T}{2T_s}\right) \right] + \zeta_{n+1} \left(1 - \frac{\Delta T}{T_s}\right) \tag{34}$$

Combining the terms yields:

$$h_{n+1} = \frac{1}{\left[1 + \left(D_{he} M \frac{d_{he}}{d_{mt}^2} \delta + \frac{D_{in}}{d_{mt}^2} d_{tk} \delta + \zeta_{n+1} \right) \Delta\tau\right]}$$

$$\left\{ h_n + D_{he} M \frac{d_{he}}{d_{mt}^2} \delta \frac{\psi}{\ell_{tk}} \Delta\tau \Delta z \left(\frac{1}{2} \phi_{I,n+1} + \sum_{i=1}^{S-1} \phi_{i,n+1} + \frac{1}{2} \phi_{S,n+1} \right) + \left(1 - \frac{\Delta T}{2T_s}\right) \left(D_{he} M \frac{d_{he}}{d_{mt}^2} + \frac{D_{in}}{d_{mt}^2} d_{tk} \right) \delta \Delta\tau + \phi_{a_{n+1}} \frac{D_{in}}{d_{mt}^2} d_{tk} \delta \psi \Delta\tau + \zeta_{n+1} \left(1 - \frac{\Delta T}{T_s}\right) \Delta\tau \right\} \tag{35}$$

where

$$w_{c_n} = \frac{w_{cp_n}}{N} \quad , \quad w_{he_n} = \frac{w_{cp_n}}{M} \quad , \quad \ell_c = K\Delta s_c \quad ,$$

$$\ell_{tk} = \ell_{he} = S\Delta z \quad , \quad \ell_r = I\Delta s_r \quad , \quad \ell_d = J\Delta s_d$$

$$\text{and} \quad \tau = n\Delta\tau$$

The initial conditions are specified at sunrise by setting the system temperature equal to the ambient temperature with no flow. The continuity of temperatures at the inlet and outlet of each system component are used as the boundary conditions. The time and space increments are chosen to satisfy the stability criteria of the numerical procedure which are obtained from the coefficients of the first term on the R.H.S. of Eqs. (27), (29), (31), and (33).

$$1 - 2\frac{\Gamma}{L_s}(f_e + K_e\gamma)\Delta\tau \geq 0 \tag{36a}$$

$$1 - \frac{w_{c_n}}{d_c^2}\frac{\Delta\tau}{\Delta s_c} \geq 0 \tag{36b}$$

$$1 - w_{cp_n}\frac{\Delta\tau}{\Delta s_{r,d}} \geq 0 \tag{36c}$$

and

$$1 - \frac{w_{he_n}}{d_{he}^2}\frac{\Delta\tau}{\Delta z} \geq 0 \tag{36d}$$

In the program, space increments have been specified. Twenty space increments were used in the collector and the connecting pipes (riser and downcomer) and 100 space increments were used in the heat exchanger and the storage tank. For longer connecting piping, 100 nodes were used. The flow diagram of the computer program is given in Fig. 4.

In order to reduce computation cost, a variable time increment was used for all cases except nighttime calculations for water as the heat transfer fluid. Note that f_e and K_e in Eq. (27) include the temperature dependent viscosities. The low viscosity of water

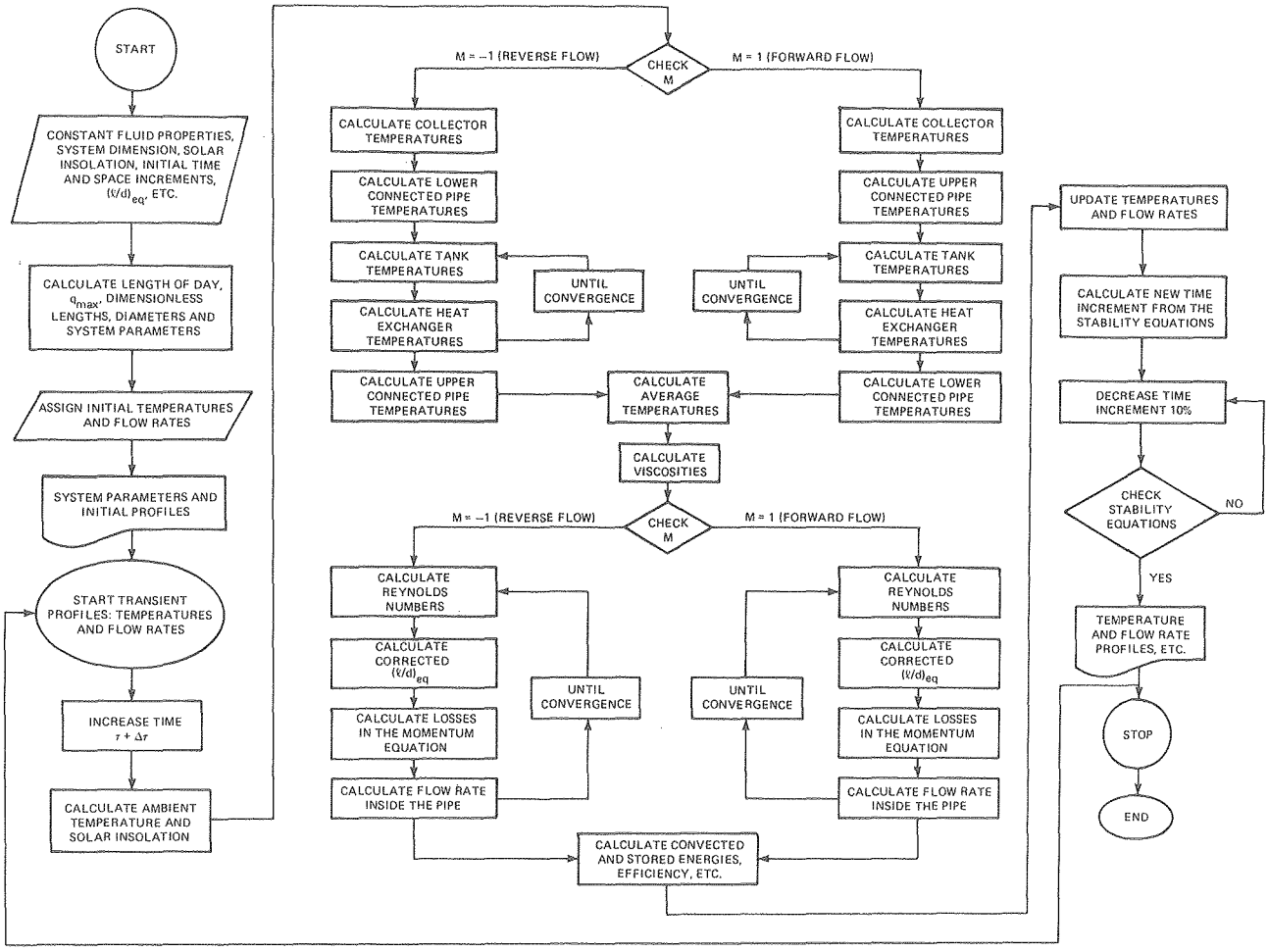

XBL 8010 – 2192 a

FIGURE 4.

results in a long characteristic damping time for fluid oscillations. It has been observed [56] that a variable time increment causes system perturbations which are critically damped in the p-glycol case but not in the water case. Therefore, a constant time step of one second was used for water runs during the night. For p-glycol and daytime water runs, the time steps were varied between 1 second and 40 seconds, as determined by the stability equations (36a-d).

Detailed measurements are currently being initiated at Lawrence Berkeley Laboratory (LBL) for purposes of validating the DLM and providing experimental data on the behavior of the various heat exchanger configurations. The experiments will attempt to carefully monitor flow rates (both forward and reverse). The predictions of the DLM have been successfully compared to the empirical method of Close [9] for the case of no draw and no heat exchanger, but additional experimental validation is clearly needed.

4. RESULTS AND DISCUSSION

The computer program was run for several days to obtain temperature and flow rate distributions. Figure 5 shows the twenty-four hour time variation of volumetric flow rate in the loop and net heat transfer to the tank for each of the first five days after start up, for the case that includes a draw from the storage tank. It is seen that at least three days are required to attain essentially steady-state performance. Unless otherwise specified, the results presented in this study correspond to "third day" results; i.e., steady-state conditions for runs which include a daily draw from the tank. If an indication is given that no draw is involved, then the results will be transient, and the day for which the results apply will be specified.

4.1 System Performance

Figure 6(a) shows DLM predictions of the twenty-four hour time variation of the volumetric flow rate in the loop and net heat transfer to the storage tank. Three flow rate curves are presented, corresponding to p-glycol in laminar flow, water in laminar flow, and water in turbulent flow. Calculation of Reynolds number for the water cases indicated that the flow in headers and connecting pipes is in the transition region ($2000 < Re < 5000$). It was decided to make two calculations, one based on the laminar flow friction coefficient, $f = 64/Re$, and the other on the Blasius turbulent friction coefficient, $f = 0.316Re^{-0.25}$ to define the upper and lower limits of the flow rate and its effect on the system performance. As is expected, the flow rate was decreased for the turbulent case (cf.

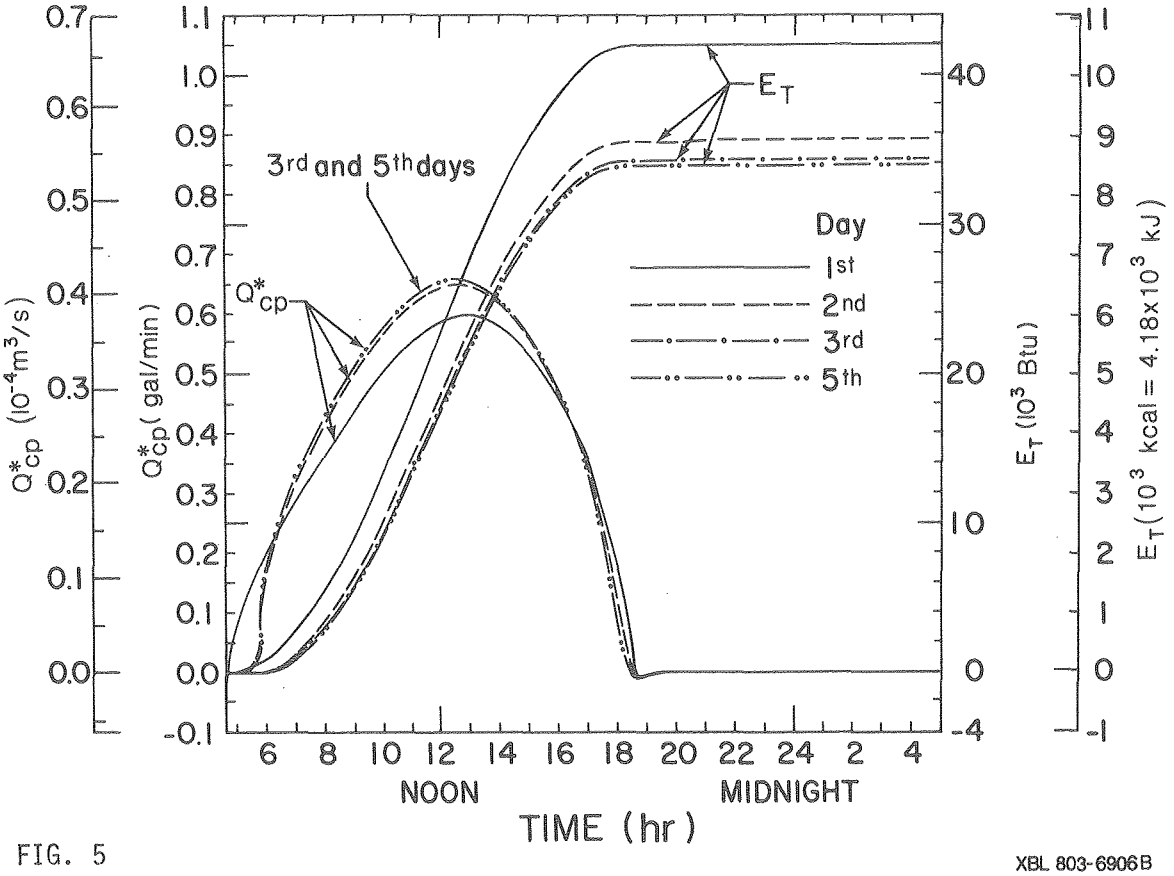

FIG. 5

XBL 803-6906B

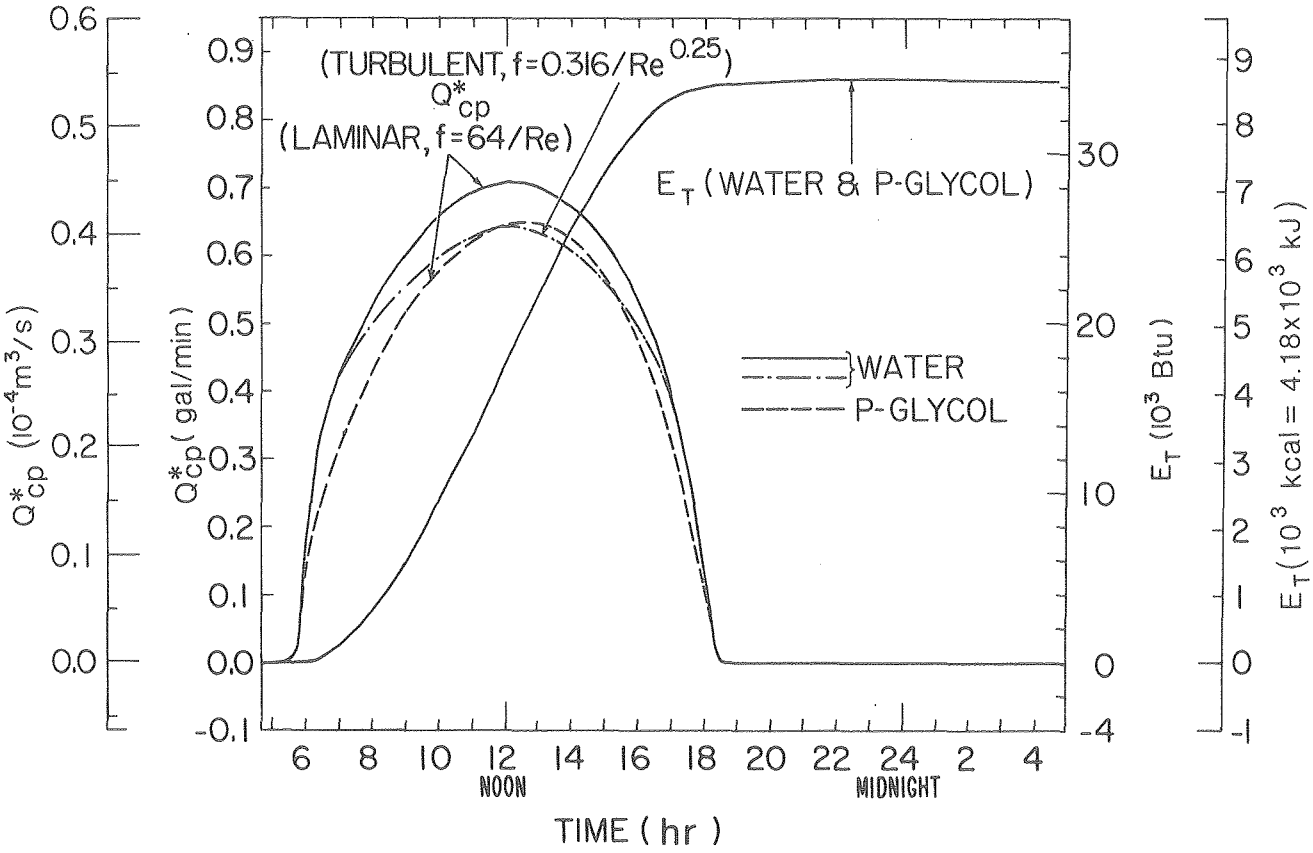

FIG. 6(a)

XBL807-7180a

Figs. 6(a) and 6(b)). The flow rates for laminar flow p-glycol and turbulent flow water are seen to be lower than the laminar flow water case, which is expected based on the higher friction. In contrast, the net heat transfer to the tank is essentially identical for the three cases. This result is somewhat surprising, since we expect the effectiveness of the heat transfer between the collector and the tank to be correlated with the flow rate of the heat transfer fluid. This counter-intuitive result can be understood in terms of the temperature distribution in the fluid loop. The large temperature rise which occurs for the p-glycol as it moves slowly up through the collector is compensated by a large temperature decrease as the fluid moves slowly through the heat exchanger. The low temperature of the p-glycol entering the bottom of the collector and the high temperature at the top of the collector result in essentially the same average collector temperature as in the water case, as will be discussed below (cf. Fig. 11(b)). Since the collector losses, which are the dominant losses of the system, are assumed to depend on the average collector temperature and to be independent of the temperature variations across the collector, the predicted system performance is essentially the same for the two fluids. In this comparison of fluids, the thermosiphon system performance is essentially invariant for 10 to 15% variations in the fluid flow rate. Simulations involving variations in the flow loop resistance predict an even larger range of flow rates over which system performance is essentially invariant; these results will be discussed below.

Figure 6(b) shows DLM predictions of the 24-hour time variation of system volumetric flow rate for the case of a traditional thermosiphon water heater with no heat exchanger operating on a day with no draw;* daytime flow fluctuations are clearly apparent. These fluctuations in the flow patterns need to be studied more carefully, particularly from an experimental point of view.

A previous work by the same authors [56] indicated incorrectly the presence of flow oscillations for water throughout the nighttime period. The simulation on which that study was based used a variable time step in order to reduce computational costs. As it was structured, the numerical method allowed an excessively long computational interval immediately after any computation which produced a very low flow velocity. Exaggerated predictions of flow velocity changes resulted from the long computational interval. In effect, the computational technique provided a random perturbation which was able to keep the system oscillating throughout the night in the case of water, the low viscosity of which results in a long characteristic damping time.

---

*Using a modified DLM wherein the heat exchanger replaced the tank with $U_{he} = U_{in}$.

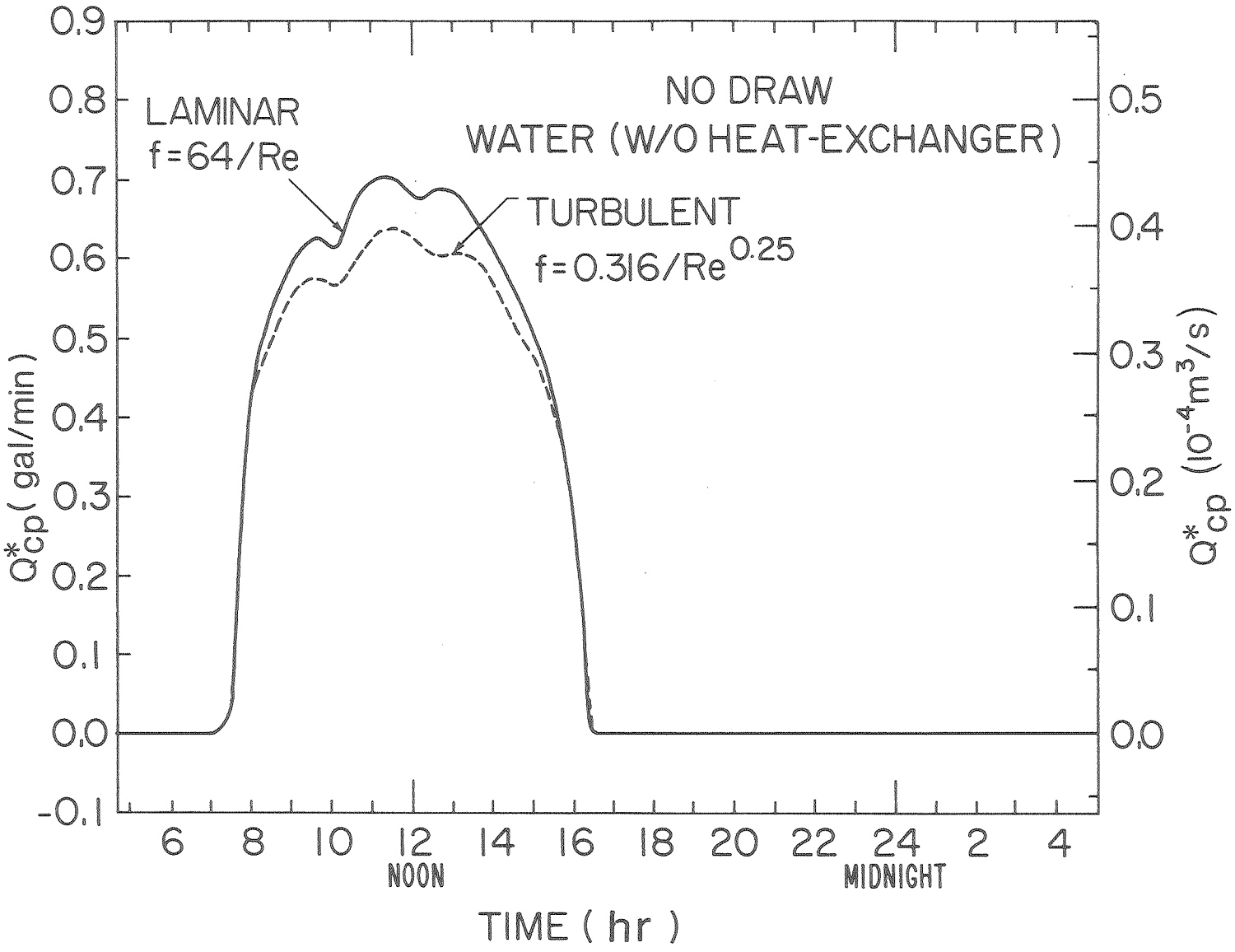

FIG. 6(b)

XBL 807-7179a

The sensitivity of the system to this "pseudo perturbation" is consistent with other predictions in the literature. For example, Zvirin et al. [30] studied the stability of the steady-state motion in an ordinary thermosiphon system by using a linearized stability equation and computing the resulting eigenvalues. They predicted oscillatory modes which could be long-lived during periods of high hot water draw from the tank--i.e., during periods when the system was significantly perturbed by the hot water draw. Furthermore, there have been numerous theoretical predictions and experimental observations of fluid flow oscillations in non-solar natural convection systems [46-53] (see Appendix). Non-oscillatory (i.e., non-reversing) flow fluctuations can also occur under certain circumstances. Experimental data from Shitzer, et. al. [31] has indicated the occurrence of daytime fluctuations.

An indication of the effect of the heat exchanger on system performance is given by Figs. 7(a) and 7(b). In Fig. 7(a) the 24-hour cumulative efficiency is plotted as a function of the variable HTR/(1+HTR), where HTR is the heat transfer ratio, defined as $(UA)_{he}/(UA_c)_c$. This ratio can be thought of as an indicator of the effect of the heat exchanger on the balance between energy transferred to the load and to the environment (through collector losses). The cumulative system efficiency is defined as the total energy transferred to the storage tank divided by the total energy incident on the system. Four points from DLM runs are used to generate each curve in Fig. 7(a), which is then extrapolated to the line HTR/(1+HTR)=1 in order to estimate the system performance for an ideal heat exchanger (infinite U_{he}). The maximum cumulative efficiency, η_{max}, thus determined is then used to set the asymptotic limit in Fig. 7(b), which shows plots of normalized (third day) system efficiency versus HTR for the cases with and without draw. Each curve is plotted using the origin and three points generated from DLM simulations. In each simulation, the assumed value of U_{he} is 170 $Wm^{-2}{}^{o}C^{-1}$ (30 Btu $hr^{-1}{}^{o}F^{-1}ft^{-2}$), and the area of the heat exchanger is chosen to correspond to 1, 2, and 3 tubes of 5.08 cm diameter (2 in. nominal). Estimates of U_{he} were based on approximate engineering calculations and assumptions about the average system temperatures and fluid flow rates. Those calculations indicate a possible range of values for U_{he}, from a high of about 170 $Wm^{-2}{}^{o}C^{-1}$(30 Btu $hr^{-1}{}^{o}F^{-1}$ ft^{-2}) to a low of about 85 $Wm^{-2}{}^{o}C^{-1}$(15 Btu $hr^{-1}{}^{o}F^{-1}ft^{-2}$). If one ignores the minor effects associated with the flow resistance of the heat exchanger, Fig. 7(b) can be used to predict the system efficiency of any values of U_{he} and A_{he}. Specifically, if the effective U_{he} for the 5.08 cm diameter tube was assumed to be 85 $Wm^{-2}{}^{o}C^{-2}$ instead of 170 $Wm^{-2}{}^{o}C^{-1}$, then there would have to be twice the number of tubes to maintain the same performance. For each point on Fig. 7(b) for which a DLM simulation was performed, the number of tubes corresponding to the two assumed values of U_{he} are indicated. The points are for specific system parameters, use patterns, and climatic conditions, so restraint should be exercised in drawing general conclusions. However, these results suggest that good

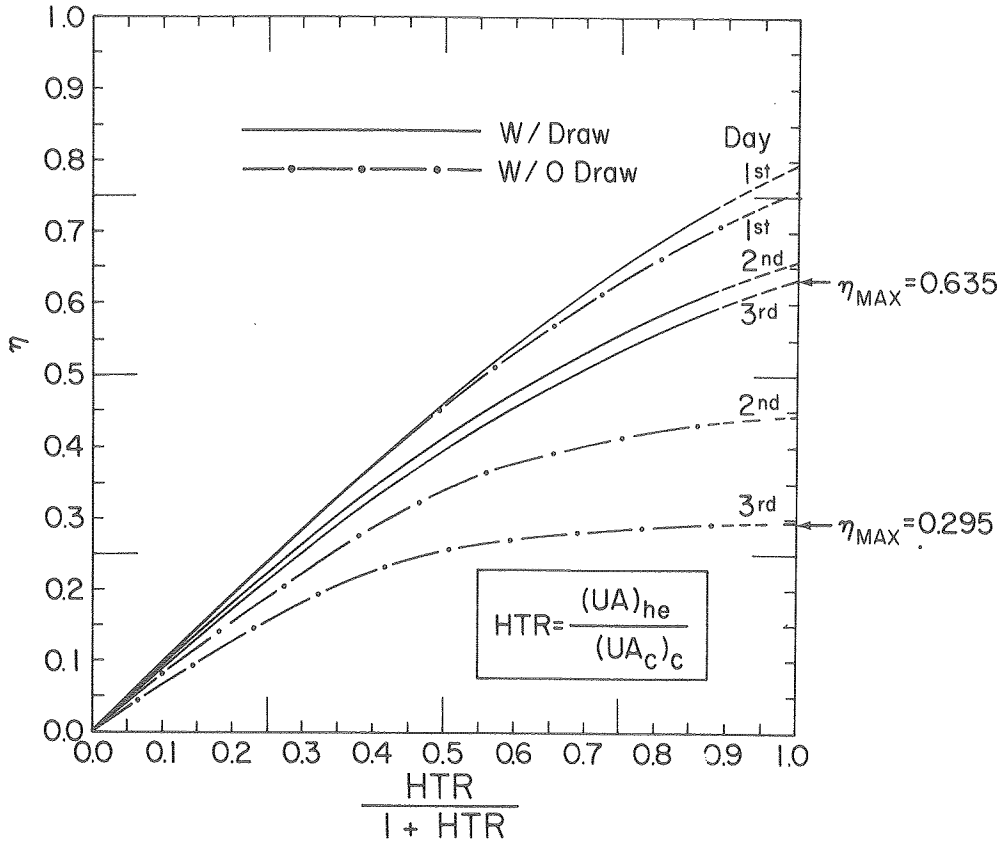

FIG. 7(a)

XBL 803-6905B

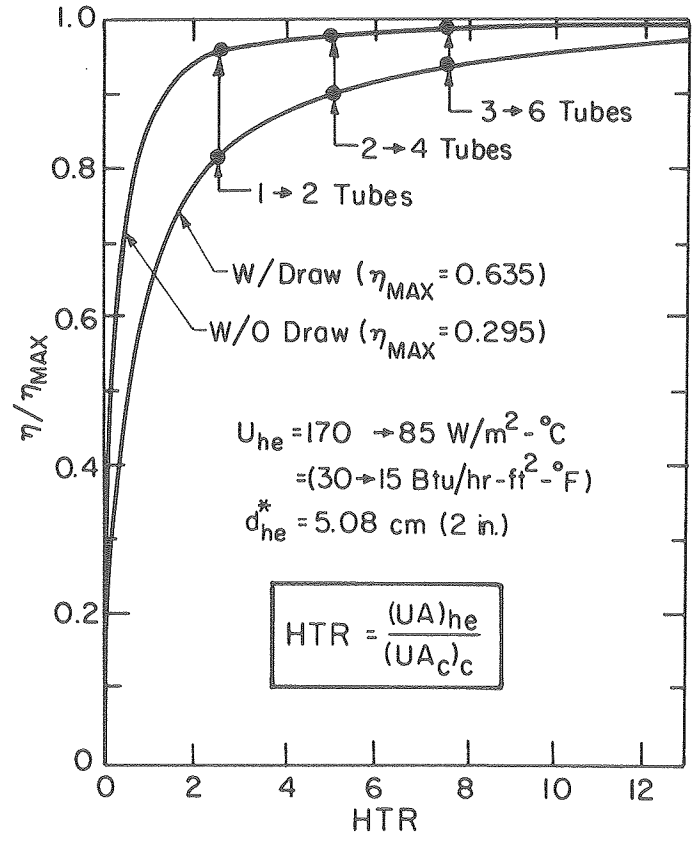

FIG. 7(b)

XBL 814-5531

system performance might be achieved by a thermosiphon with a simple heat exchanger composed of straight tubes, using p-glycol in the collector loop.

The predicted effect of tank stratification on the system performance is shown in Fig. 8. The tank temperature distribution is an extremely complicated function of the energy delivery, the energy loss, and the mixing effect of supply water surges. As explained before a simple tank model is used to reduce computation costs. The DLM predictions show that a condition of maximum tank stratification ($11^{o}C$) results in a system performance about 10% better than for the condition of a fully mixed tank. This result is attributable both to the superior heat transfer associated with the colder fluid near the tank bottom and to the availability of hotter water to be drawn off at the top of the tank.

The predicted effects of tank elevation relative to the collector are shown in Fig. 9. The daytime flow rate decreases with decreasing tank elevation as a result of reduced buoyancy forces. The reverse flow at night is negligible if the bottom of the tank is above or even with the top of the collector, but becomes substantial if the bottom of the tank is placed below the top of the collector. The deleterious effect of the reverse flow is apparent from the nighttime decline of the cumulative energy transfer; the nighttime losses increase with the rate of reverse flow. System performance is shown to be insensitive to the daytime flow rate. The daytime energy transfer is the highest for the tank in the lowest position ($y = -1.22$ m). This result is attributable to the lower system temperatures which result from the nighttime reverse-flow losses.

The effects of flow resistance are shown in Figs. 10(a) and 10(b). Figure 10(a) again shows that, over a large range, a decrease in the flow rate has only a small effect on the system performance. The energy transfers are indistinguishable for collector tube sizes greater than or equal to the nominal 1/4 in. diameter (I.D. = 0.32 in. = 0.80 cm). Collector tubes of nominal 1/8 in. diameter (I.D. = 0.19 in. = 0.48 cm) produce a slight reduction in system performance. Figure 10(b) shows the effects of connecting pipe diameter for a total connecting pipe length (riser plus downcomer) of 8.4 m (27.5 ft). Compared to the connecting pipe, the collector tubes are shorter and present several parallel paths to accommodate the flow. Consequently, pronounced performance reductions appear at larger diameters for the connecting pipes than for the collector tubing. For the system configuration being simulated, the performance reduction in going from 1/4 in. to 1/8 in. (nominal) collector tubing is about the same as the performance reduction in going from 1 in. to 1/2 in. (nominal) connecting pipe. Figures 10(a) and 10(b) show that although tubing diameter is not a negligible factor, flow-independent behavior can be achieved at fairly modest diameters for both the collector tubing and connecting pipe. The results also indicate the desirability of minimizing the

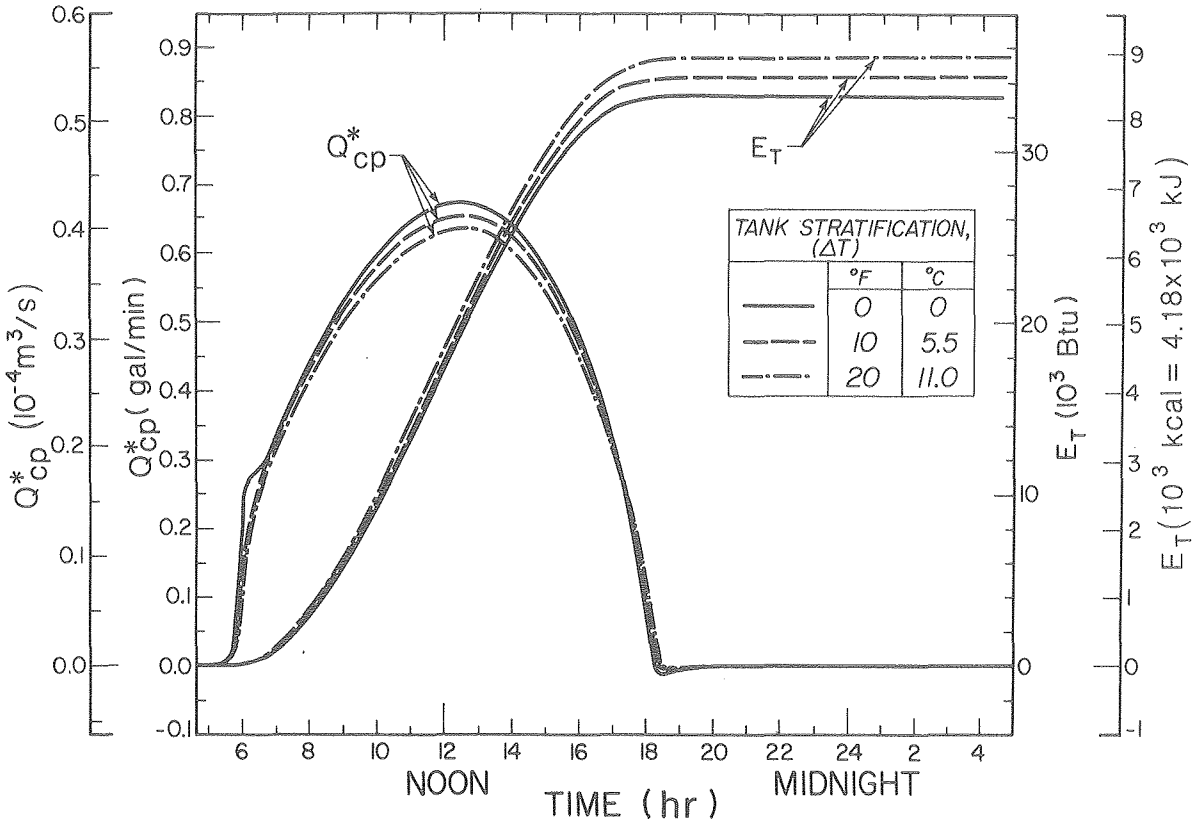

FIG. 8

XBL 803-523b

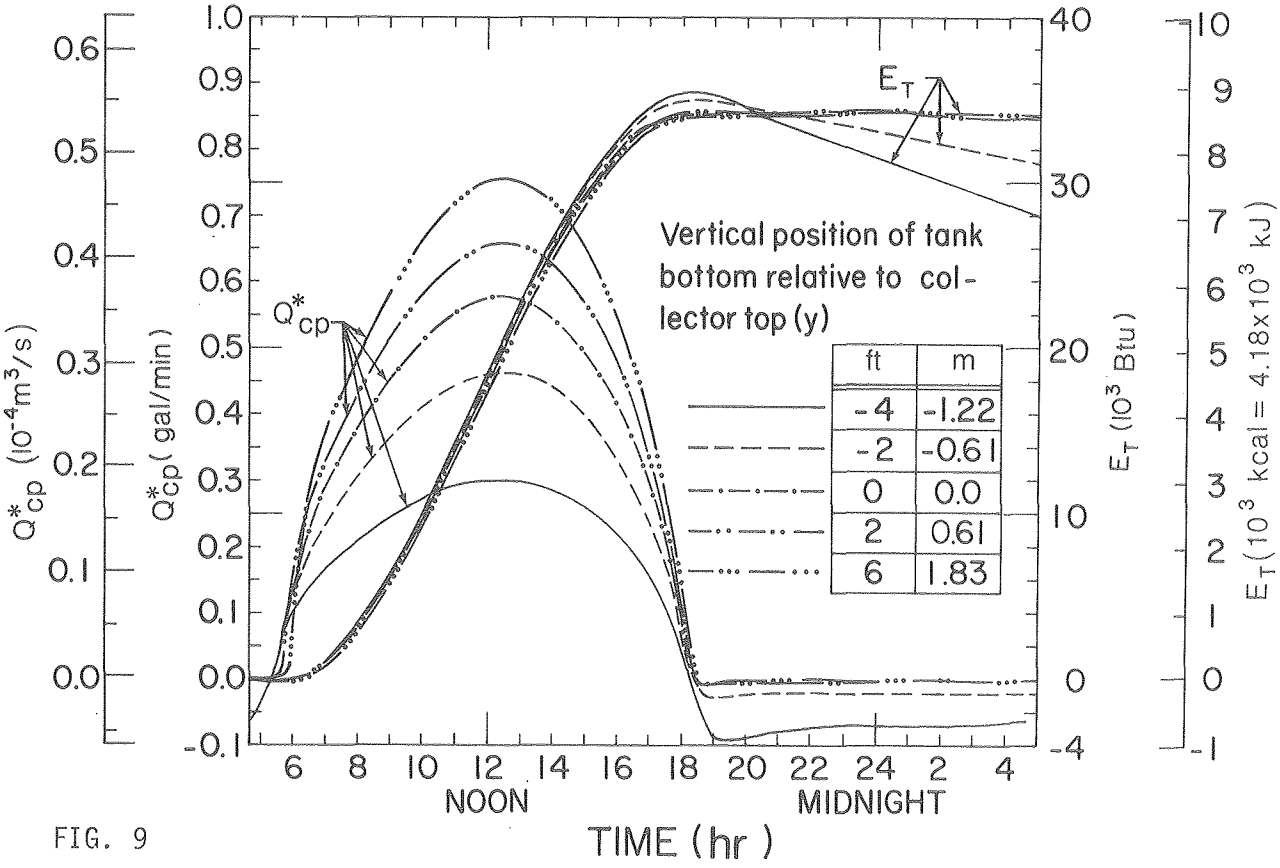

FIG. 9

XBL 803-6903B

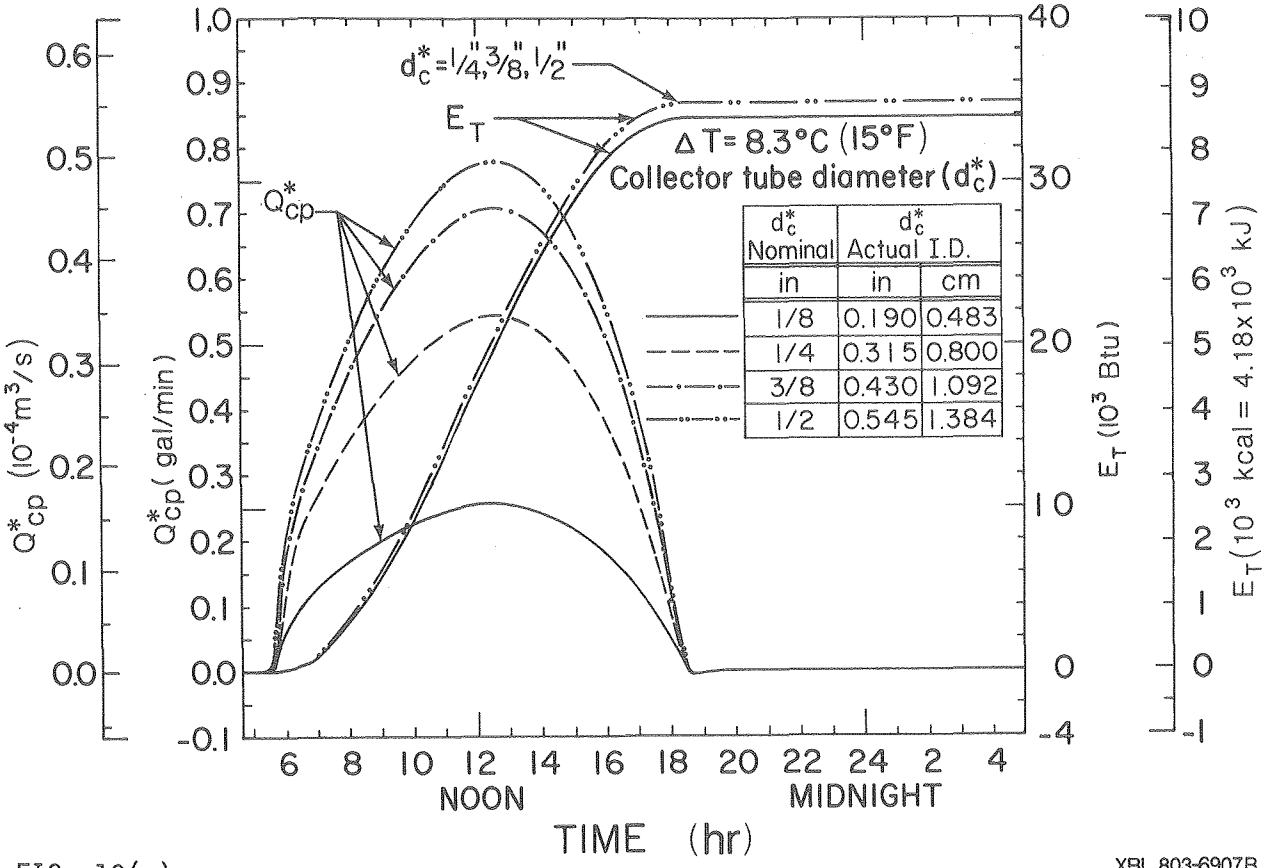

FIG. 10(a)

XBL 803-6907B

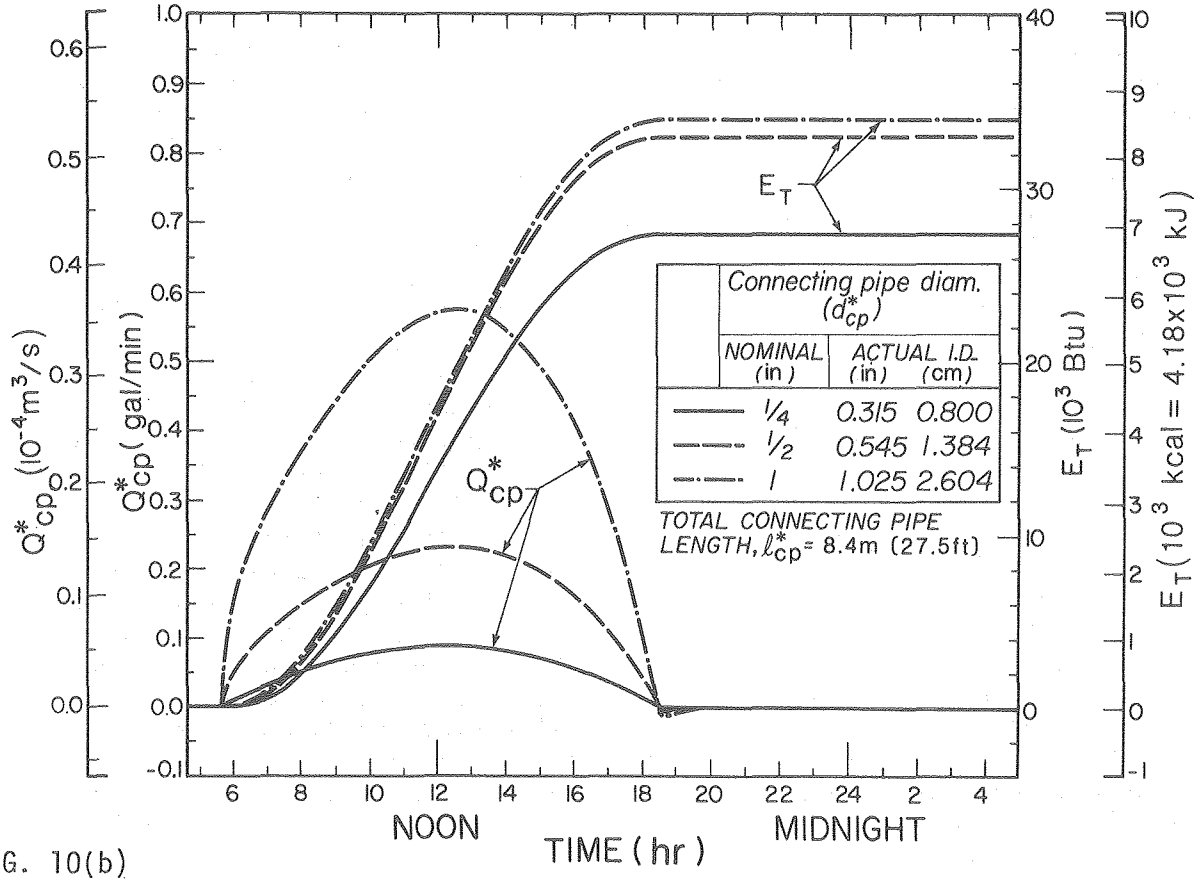

FIG. 10(b)

XBL 803-522 b

connecting pipe lengths since economies can be realized from both the reduced length and the reduced diameter which can be tolerated without performance reductions.

4.2 Temperature Profiles

Figures 11 through 16 show typical system temperature profiles for various tank elevations, heat transfer fluids, and tank stratifications. The following discussion of those figures illustrates how the detailed results from the DLM can be useful in understanding the system performance.

Figures 11(a) - 11(c) show the temperature of the heat transfer fluid as a function of height in the loop, at three different times of the third day. The correspondence between temperatures and points in the system can be established with reference to points A, B, C, and D which are labeled on each temperature plot and also on the simple system schematic at the top of the figure. Temperature curves for the collector and heat exchanger are solid and for the connecting pipes are dashed. Since fluid density is assumed to be a linear function of the temperature, the net integrated area under the temperature curve is proportional to the net buoyancy driving the fluid around the loop. If the area integration is performed by moving around the loop in the sequence A to B to C to D, then a positive integral is associated with forward flow and a negative integral with reverse flow. The plots of temperature versus height are simple closed figures during daytime collection periods (e.g., at 9 a.m. and 3 p.m.), but are more complex, with crossovers, during periods of reverse flow (e.g., at 3 a.m.).

In Fig. 11(a), temperature versus height curves are plotted for three different positions of the tank relative to the collector. For the case with the bottom of the tank four feet below the top of the collector, $y = -1.22$ m, (top diagram), the 3 a.m. plot shows a negative area which substantially exceeds the positive area, indicating a substantial net negative buoyancy force to drive reverse flow. For the case with the bottom of the tank even with the top of the collector (middle diagram) and with the bottom of the tank 1.83 m above the top of the collector (bottom diagram), the 3 a.m. plots show negative areas which are also almost completely balanced by the positive areas, indicating that the net negative buoyancy force driving reverse flow is small. These results are entirely consistent with the reverse-flow results presented in Fig. 9. The daytime temperature plots shown in Fig. 11(a) are also consistent with the forward-flow results and performance curves presented in Fig. 9. As the tank elevation increases, i.e., as we move downward through the diagrams in Fig. 11(a), the positive area inside the daytime plots increases, indicating a higher buoyancy force driving the flow, with a consequent higher flow rate. In contrast, as the tank height is increased, the temperature differences across the collector and the heat exchanger decrease but the average collector temperature remains nearly constant. Over the range of system configurations depicted in Fig. 11(a), multiplying the daytime flow rate times the collector temperature difference at a given time produces essentially the same value for each tank height. The fact that the average collector temperature remains constant explains the highly similar daytime performance curves depicted in Fig. 9.

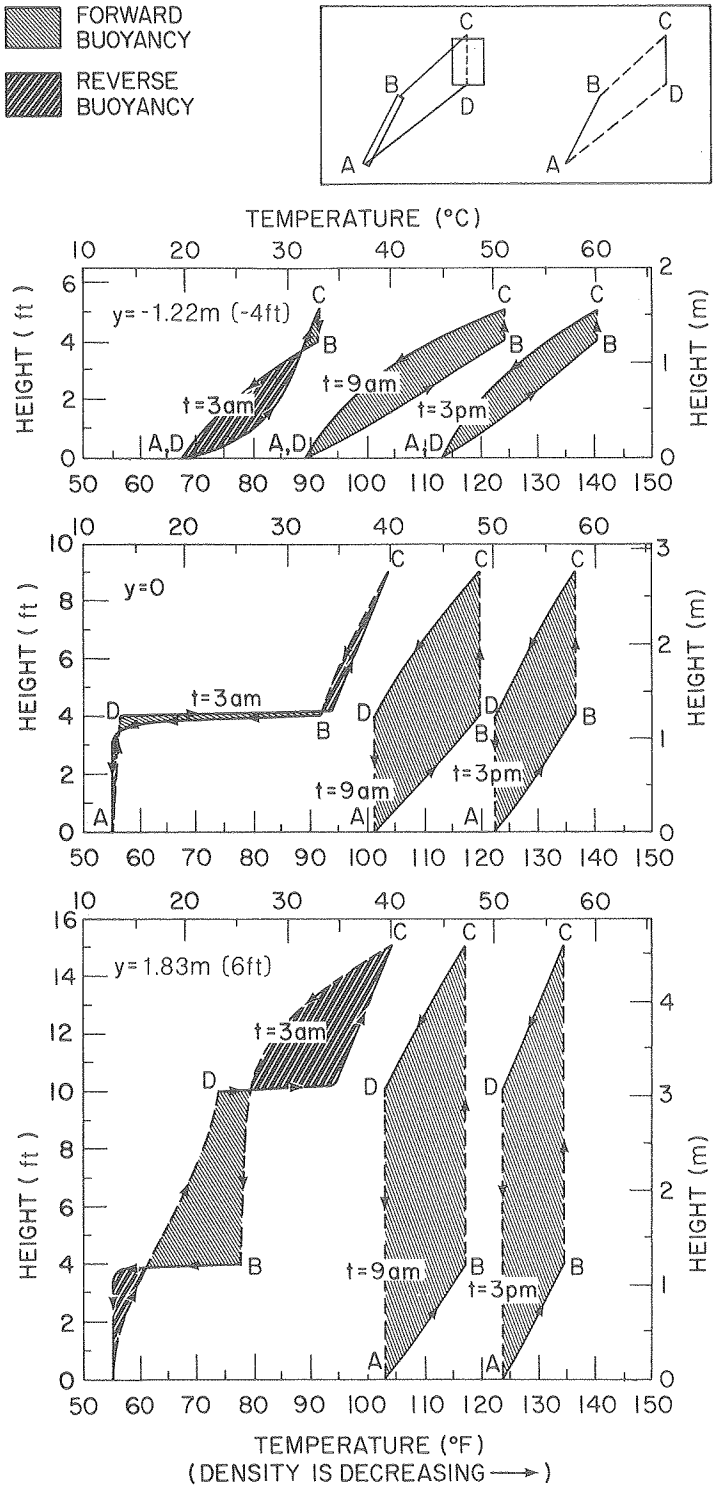

FIG. 11(a)

XBL 806-7154A

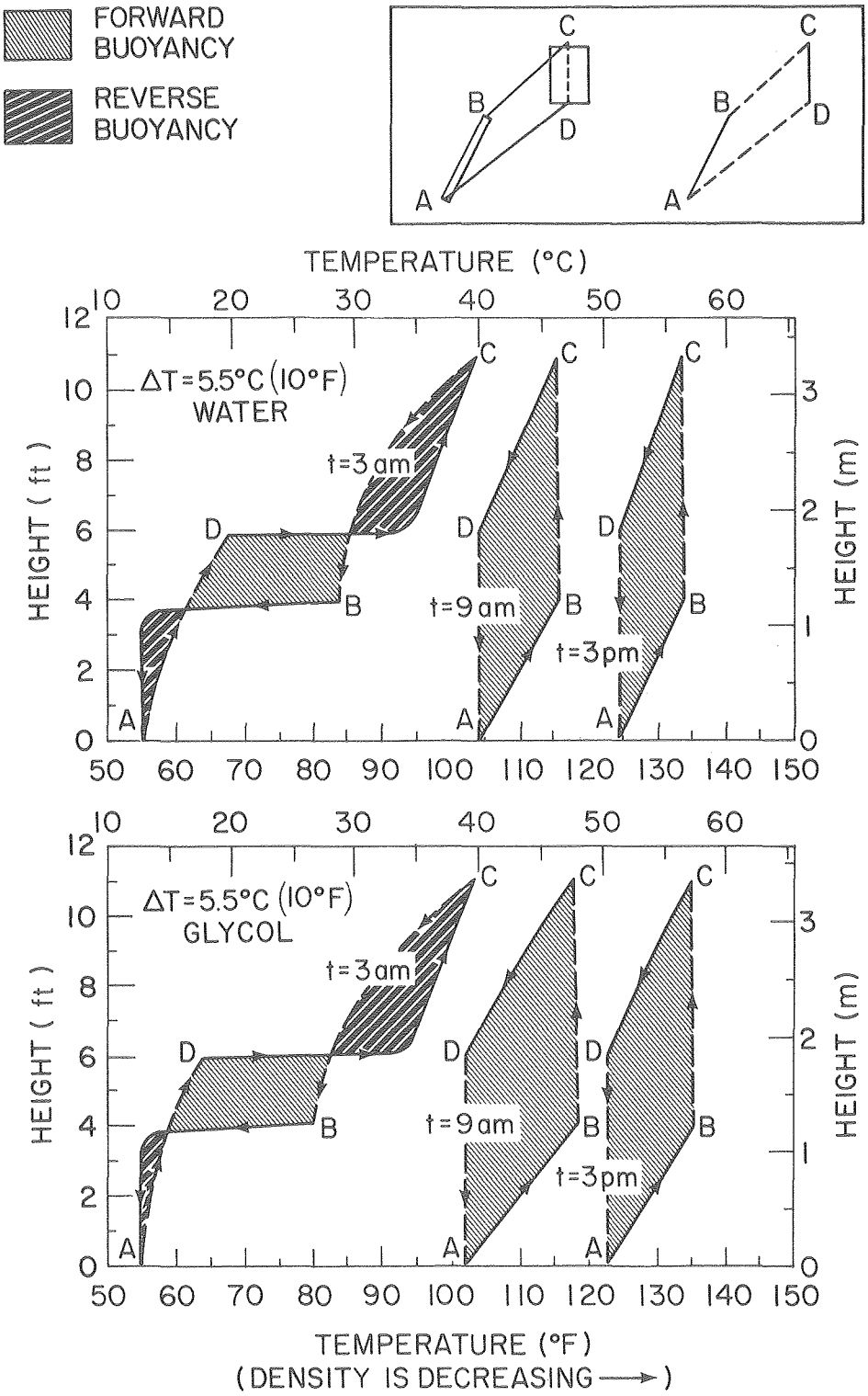

FIG. 11(b)

XBL 8010-2174 A

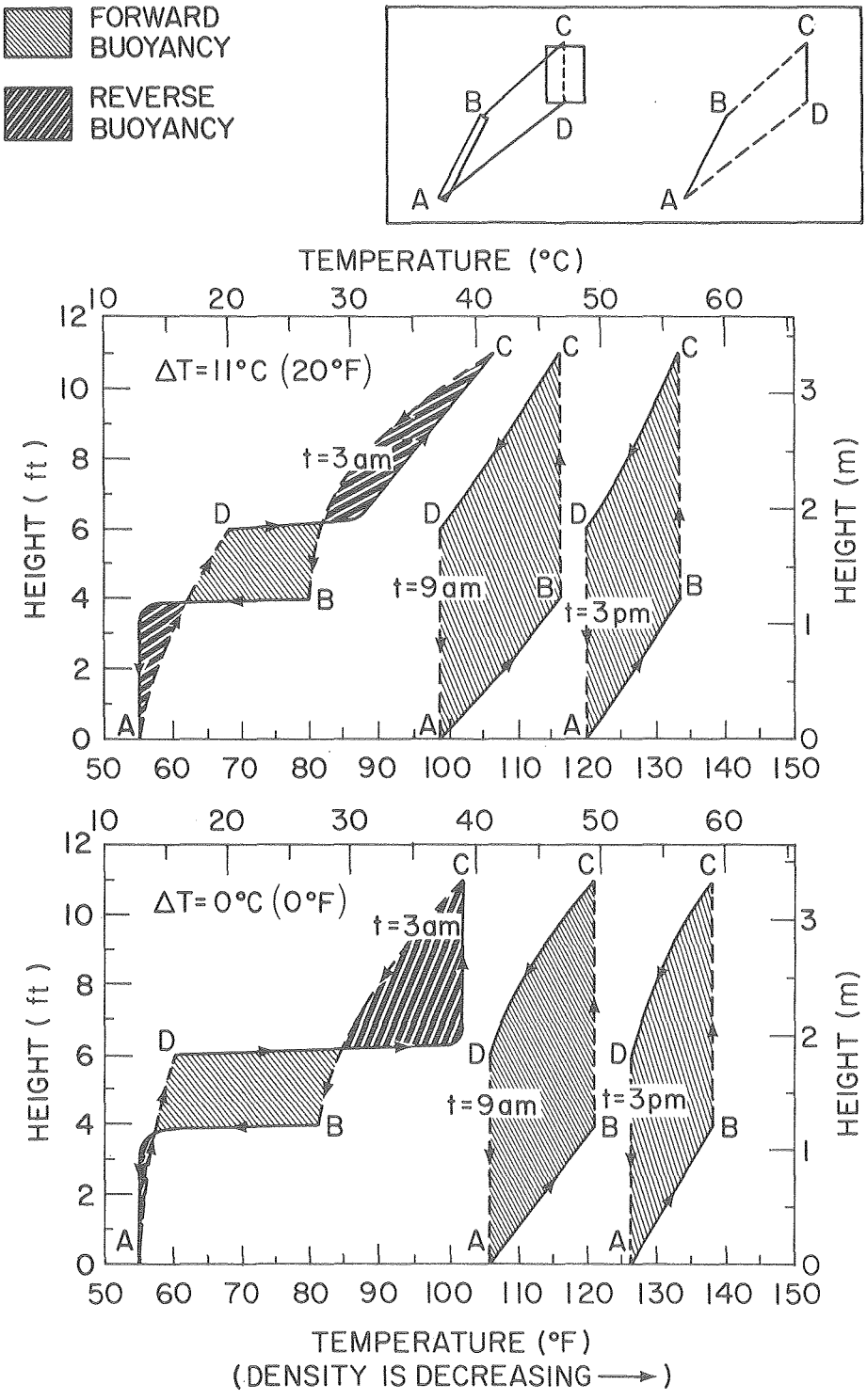

FIG. 11(c)

XBL 806-7153A

In Fig. 11(b), the top diagram shows temperature plots for a system using water as the heat transfer fluid in the loop, and the bottom diagram shows the corresponding plots for an identical system using p-glycol as the heat transfer fluid. As discussed in the section on system performance, p-glycol has a higher viscosity than water which results in a lower flow rate and a larger temperature difference across the collector. The bottom diagram in Fig. 11(b) shows that this increase in temperature difference also results in a larger positive area during the daytime collection periods (9 a.m. and 3 p.m.). This larger positive area, along with p-glycol's higher coefficient of thermal expansion, results in a buoyancy force which is substantially larger than that of water circulating in the loop. However, p-glycol's higher viscous resistance more than offsets the buoyancy force advantage, resulting in a flow rate which is somewhat lower than in the water case. As mentioned earlier, the large temperature rise which the p-glycol experiences as it moves up through the collector just compensates for the low flow rate, resulting in a collection efficiency which is almost identical to water.

Figure 11(c) shows the effect of tank stratification on the temperature profile inside the heat exchanger. As expected, for the case with a large tank stratification ($\Delta T = 11^{o}C$), the rate of temperature drop with vertical coordinate is smallest at the top of the heat exchanger, where the high tank temperature limits the heat transfer rate, and is largest at the bottom of the heat exchanger, where the low temperature of the tank water results in a high heat transfer rate. In the case of no tank stratification ($\Delta T = 0^{o}C$), the rate of change of temperature with respect to the vertical coordinate is largest at the top of the heat exchanger where the hot fluid entering the heat exchanger transfers its heat rapidly to the cooler tank water, and is smallest at the bottom of the heat exchanger where the cooled fluid is transferring heat at a lower rate. The $11^{o}C$ tank stratification results in a performance which is about 10% better than for $0^{o}C$ stratification (cf. Fig.8), partly because of the superior heat transfer associated with the colder tank bottom, and partly because of the availability of hotter water to be drawn off the top of the tank. For both conditions of stratification, the nighttime temperature distribution in the heat exchanger mirrors the assumed tank temperature distribution everywhere except at the bottom, where the trickle of fluid entering the heat exchanger reduces the temperature below the adjacent tank temperature. This cooling effect is limited to a small region, because of the small reverse flow rate. One of the limiting features of the tank model, which specifies stratification as an input parameter, is the persistence of a constant tank stratification throughout nighttime hours. The energy flux on the tank at night is substantially smaller than during the daytime, when the cold supply water and heat input from the exchanger are driving stratification.

Temperature differences (ΔT) across the collector and the heat exchanger are plotted in Figs. 12 and 13 for different tank and collector separations. The sudden increase in the collector and heat exchanger ΔT at the end of the day corresponds to the onset of the reverse flow. Hot fluid in the riser reverses direction and enters the collector top

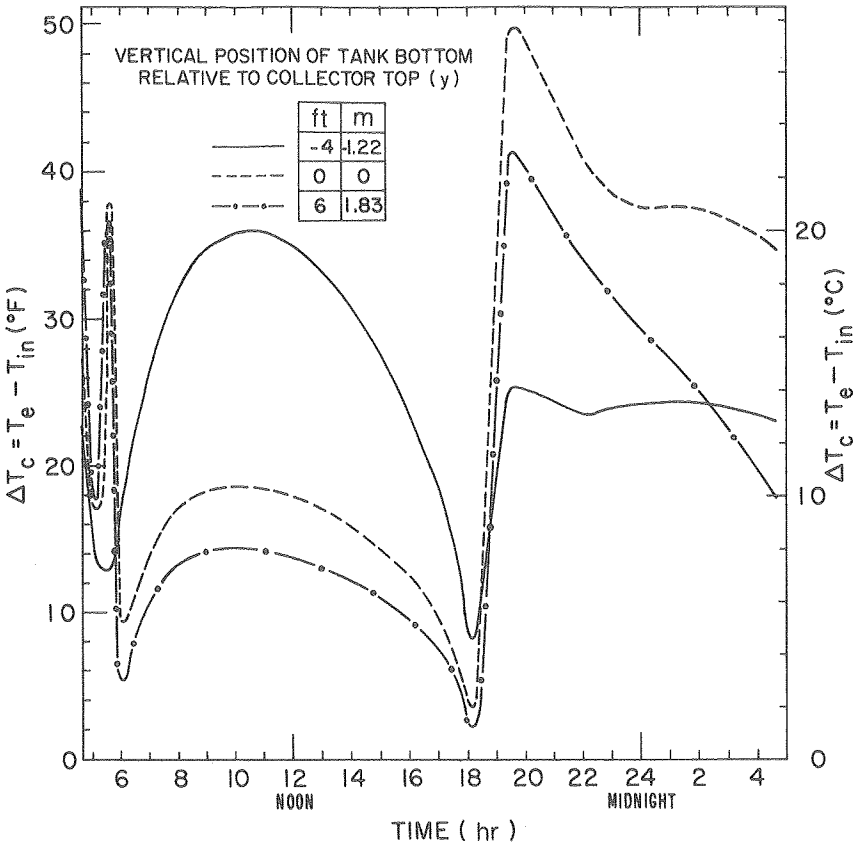

FIG. 12

XBL 806-7159A

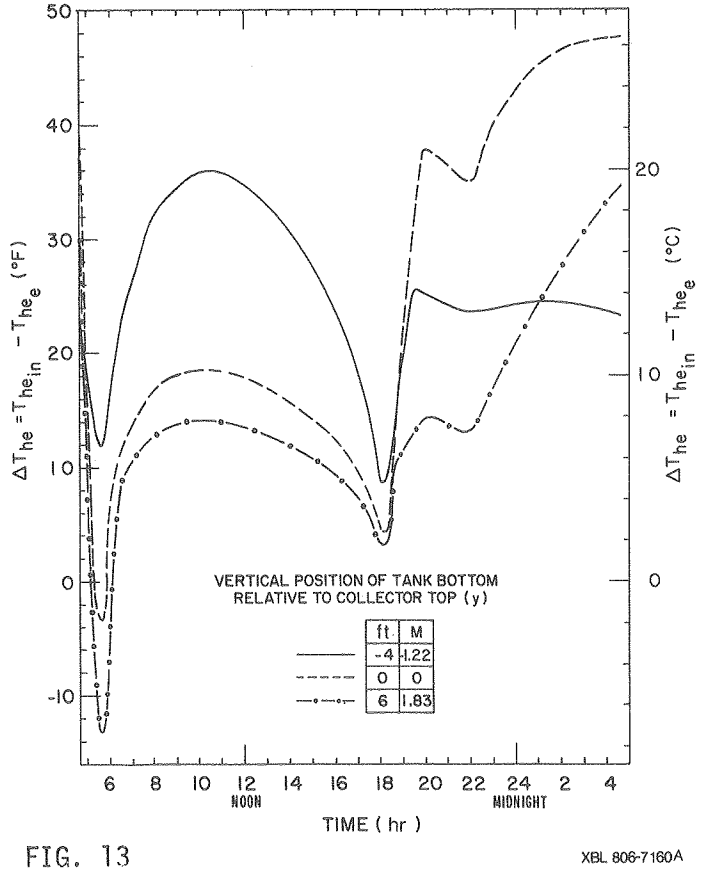

FIG. 13

XBL 806-7160A

while cold fluid from the downcomer enters the heat exchanger bottom resulting in an increase in the temperature difference across these components. The minimum value of ΔT in the early morning (about 5 a.m.) corresponds to the onset of forward flow. When the forward flow resumes in the system, the ΔT initially increases due to the incoming cold fluid from the downcomer into the collector. As the cold fluid moves up through the collector, the fluid leaving the collector exit becomes cooler than the fluid that was there earlier and causes a decrease in the temperature difference. A similar discussion applies to the temperature difference across the heat exchanger (cf. Fig. 13).

Figure 14 shows the average temperature difference between the heat exchanger and the storage tank. During the daytime the difference is positive, indicating energy transfer from the heat exchanger to the storage tank. During the night the difference is negative, indicating energy transfer from the tank to the heat exchanger, which is characteristic of the reverse flow. During the day the energy transfer for all cases is almost the same, but there is a substantial change during the night (cf. Fig.14 for the cases, y = 1.83 m and -1.22 m).

Figure 15 shows the difference between the average collector temperature and the ambient temperature as a function of time. This difference is proportional to the collector energy loss. For the cases shown, there is negligible difference in collector loss during the daytime. However, during the night for the low separation case (y = -1.22 m), the high reverse flow rate causes the collector temperature to be significantly higher than the ambient temperature.

The average temperature difference between the collector and the heat exchanger is plotted in Fig. 16 for different tank separations. During the daytime for the cases y = 0 and y = 1.83 m, the collector and the heat exchanger average temperatures are very close. As mentioned before this behavior is well established for common thermosiphons (no heat exchanger and no draw) [9].

5. CONCLUSIONS

A number of conclusions can be drawn from these studies. However, the following major assumptions (in addition to those inherent in the model) and the limited scope of this study should be emphasized when analyzing these conclusions: The baseline model consisted of a residential sized system (0.302 m^3 tank, 3.9 m^2 of collector) which included a vertical tank with straight bare 2 in. diameter copper heat exchanger tubes, 60% p-glycol heat transfer fluid, and two internally manifolded tube-in-sheet single glazed selective surface collectors, 1 in. diameter connecting pipes and tank, 0.61 m above the collector. The heat exchanger overall heat transfer coefficient was assumed to be constant (170 $Wm^{-2}{}^{o}C^{-1}$) and the system was modelled for a single warm day, with a draw profile shown in Fig. 3.

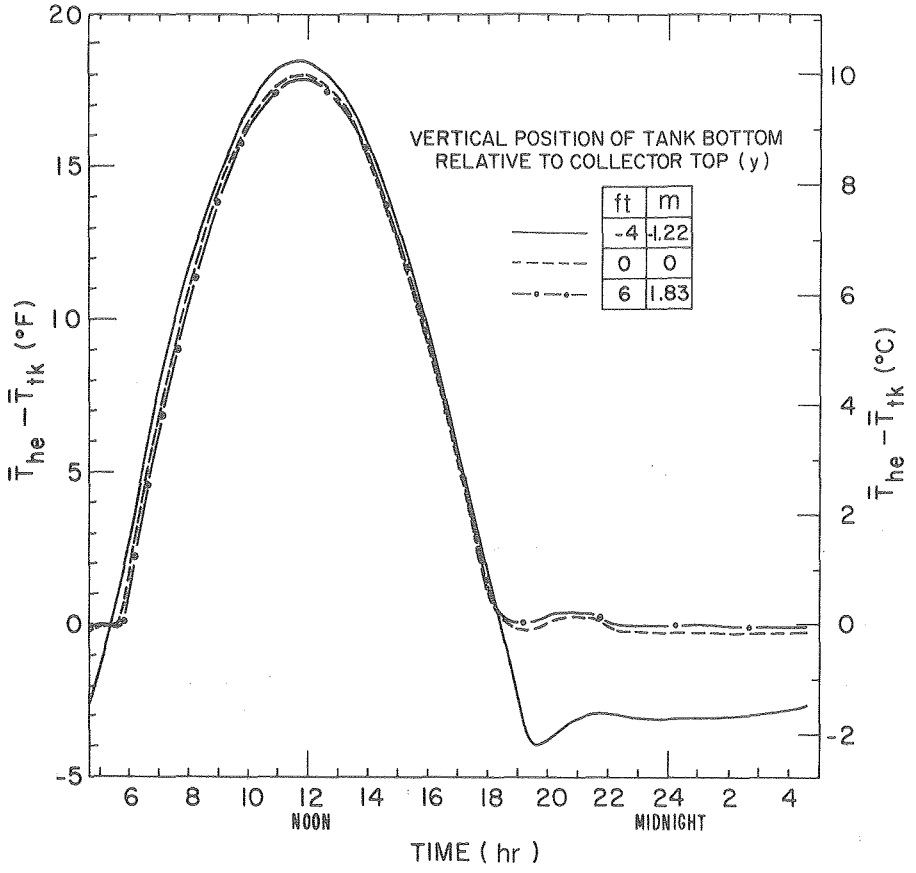

FIG. 14

XBL 806-7158 A

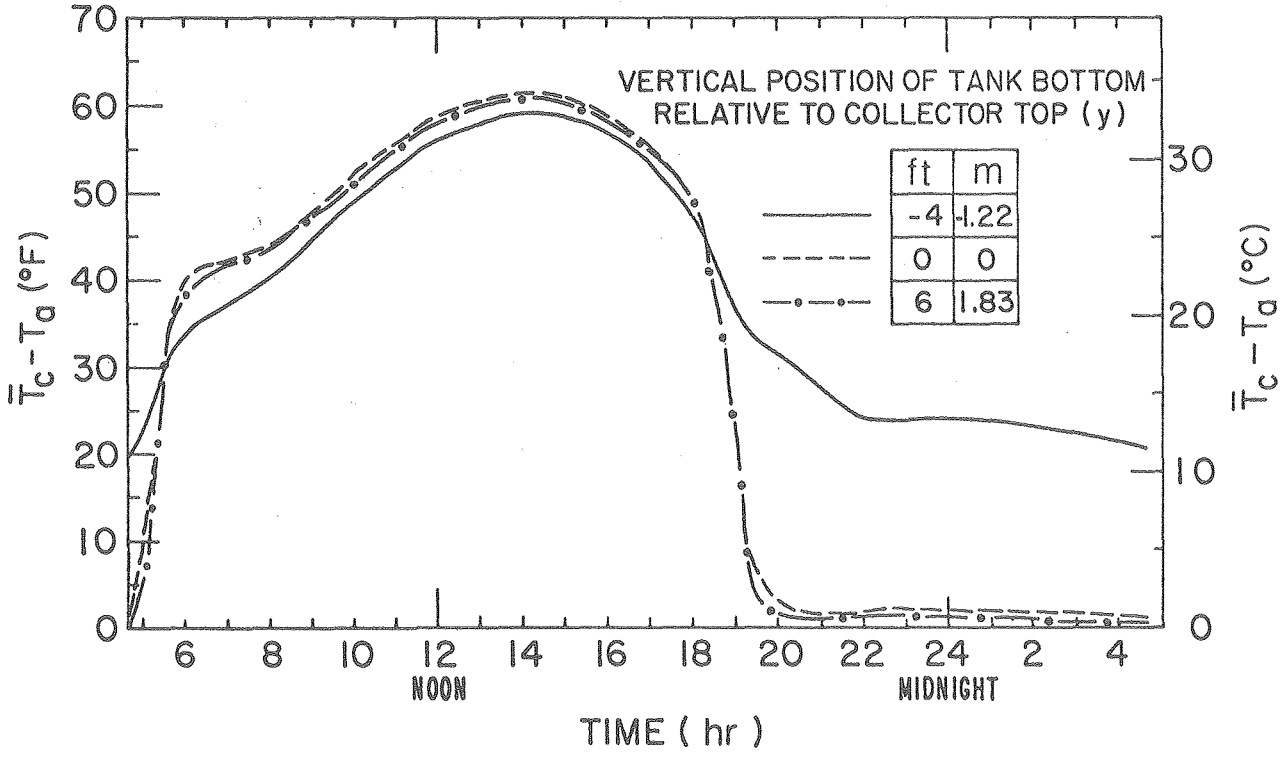

FIG. 15

XBL 806-7157 a

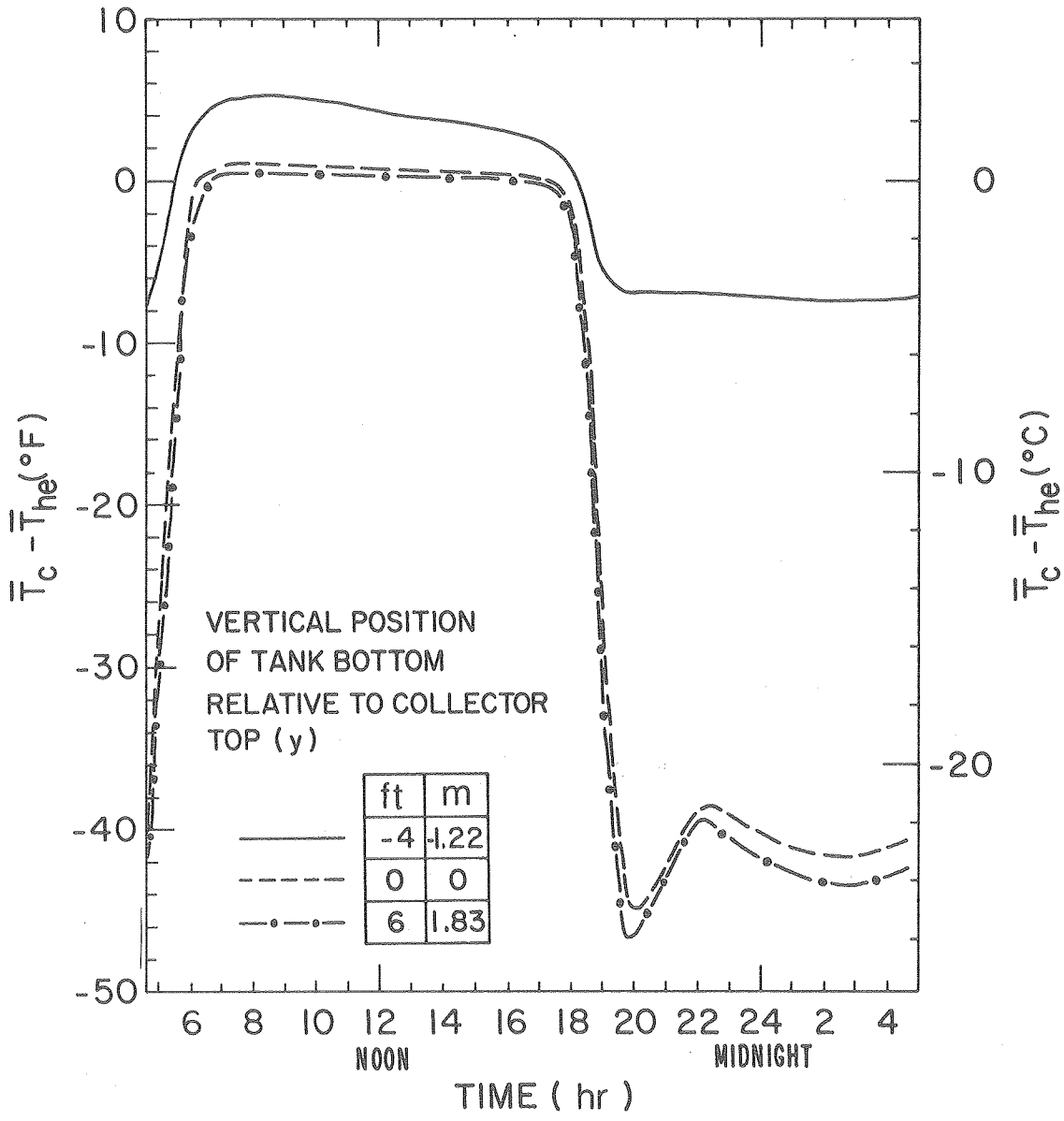

XBL 806-7156 A

FIG. 16

The performance predictions for three heat exchanger tubes of diameter 5.08 cm (2in. nominal) indicate that the system performance would be on the order of 90% of that expected from a standard thermosiphon without a heat exhanger, for the design day simulated. Although annual performance has not been calculated, this design day result suggests that there might exist a practical range of heat exchanger sizes for this particular system configuration.

An analysis was made of the performance sensitivity of this system to various design parameters from which the following conclusions were drawn:

(1) Comparing the performances for different assumed linear tank stratifications (ΔT), it was shown that the system performance is relatively insensitive to the tank stratification. Therefore detailed tank models may not be necessary. The daily cumulative energy for no stratification ($\Delta T = 0$) was about 10% less than for $11^{o}C$ stratification. The maximum flow rate was decreased about 8%.

(2) Varying tank elevation relative to the collector showed no significant effect on the 24 - hour performance until the bottom of the tank was below the top of the collector. The daytime performance, however, was unaffected by the tank elevation. The substantial losses for the lower tank elevations result from reverse flow at night that is suppressed when the bottom of the tank is above or even with the top of the collector. These losses could also be eliminated by using a suitable one-way valve.

(3) Studies of different collector tube diameters showed that diameters between 1/4 in. and 1/2 in.,while causing a difference in maximum flow rate of about 30%,had a negligible effect on the end of day performance. When the tube diameter is reduced to 1/8 in., the daily cumulative energy gain was reduced by only 2%. This result indicates that the system performance is insensitive to the collector flow resistance for most commonly available tube-in-sheet collectors.

(4) When connecting pipe diameters were reduced from 1 in. to 1/4 in. flow rate decreased dramatically by 87% and the end of day performance was reduced by 16%. 1/2 in. connecting tubes reduced maximum flow rate by 60% but the performance was reduced by only about 3%. This indicates that the performance of this system is relatively independent of flow rate as well as the connecting pipe flow resistance unless the tube sizes are reduced to uncommonly small sizes.

To fully establish the technical and economic viability of this type of freeze-protected thermosiphon water heater, the following additional studies are necessary:

(1) Experimental validation of the Detailed Loop Model (DLM).

(2) Development of a simplified algorithm to study the annual performance of thermosiphons with heat exchangers in various climates, and in particular, the generalization of the dependence on fluid properties.

(3) Comparison of the performances of vertical and horizontal tanks.

(4) Design of heat exchangers for thermosiphon systems with vertical and horizontal tanks.

(5) Comparison with forced convection systems.

(6) Effect of simplifying assumptions, such as constant U_L, F', U_{he}, etc.

NOMENCLATURE

A	cross-sectional area
A_{cc}	surface area of collector
B	header loss modifier, Eq. (5d)
B'	header loss modifier, Eq. (5d)
c	specific heat
d	dimensionless diameter
d_{mt}	modified storage tank diameter, Eq. (15b)
D_c	collector heat transfer parameter, Eq. (18b)
D_{he}	heat exchanger heat transfer parameter, Eq. (18c)
D_{in}	insulation loss parameter, Eq. (18d)
E_T	cumulative energy transfer to storage tank
f	friction coefficient
f_e	equivalent friction coefficient, Eq. (5b)
F'	plate efficiency factor
g	acceleration of gravity
Gr_m	modified Grashof number, Eq. (19a)
h	unknown time dependent function in the storage tank temperature profile, Eq. (13)
H	dimensionless height of the system

HTR	heat transfer ratio = $(UA)_{he}/(UA_c)_c$
K	friction loss coefficient
K_e	equivalent friction loss coefficient, Eq.(5c)
ℓ	dimensionless length
ℓ_{cp}	dimensionless total length of connecting pipes (riser and downcomer)
$(\ell/d)_{eq}$	equivalent length of a resistance to flow in pipe
L_s	dimensionless system parameter, Eq. (5a)
L_T	characteristic system length, Eq. (16b)
M	total number of heat exchanger tubes
N	total number of collector tubes
p	pressure
P	dimensionless length of day (total solar time)
q	heat flux
Q	volumetric flow rate
Re	Reynolds number
Re_{ch}	characteristic Reynolds number, Eq. (19b)
Ri	Richardson number, Eq. (19c)
s	dimensionless space coordinate along the loop
Δs	dimensionless space increment in finite difference equations
S_t	daily total solar radiation
t	time
T	temperature
T_{amp}	difference between maximum and minimum temperature during a day
T_{ave}	average temperature during a day
ΔT	temperature difference between top and bottom of storage tank

U	overall heat transfer coefficient
U_c	collector overall heat transfer coefficient, $U_c = F'U_L$
U_L	overall collector loss coefficient
v	velocity
V	characteristic velocity, Eq. (17); total volume of storage tank
$\dot{V}$	amount of draw
w	dimensionless volumetric flow rate (or velocity)
x	horizontal position of tank center relative to collector top
y	vertical position of tank bottom relative to collector top
z	dimensionless vertical space coordinate
Δz	dimensionless vertical space increment in finite difference equations

Greek symbols

α	normal absorptivity of collector absorber plate; horizontal angle between riser and collector top
β	thermal expansion coefficient
γ	connecting pipe parameter, Eq. (18i)
Γ	thermosiphon convection parameter, Eq. (18a)
δ	fluid parameter, Eq. (18e)
ζ	draw parameter, Eq. (18g)
η	cumulative efficiency
θ	collector tilt angle
μ	absolute viscosity
ξ	collector geometry parameter, Eq. (18h)
ρ	density

$\Sigma(\ell/d)_{eq}$ summation of equivalent length of a resistance to flow in a specified system component

τ dimensionless time, normal transmissivity of collector cover plate

$\Delta\tau$ dimensionless time increment in finite difference equations

ϕ dimensionless temperature

ψ solar radiation parameter, Eq. (18f)

Ω horizontal angle between downcomer and collector bottom

Subscripts

a ambient

c collector tube

ch characteristic

cp connecting pipes (riser and downcomer)

d downcomer tube

e exit

eq equivalent

h header

he heat exchanger

i space step in finite difference equations; instantaneous

in inlet; insulation

I location at the end of riser

J location at the bottom of collector

K location at the top of collector

max maximum

n time step in finite difference equations

o circulating fluid properties at reference temperature

r riser tube

s supply

sr solar radiation

S location at the end of heat exchanger

tk storage tank

w water

Superscripts

* dimensional

- average

REFERENCES

(1) Chauhan, R.S. and Kadambi, V., "Performance of a Collector-Cum-Storage Type of Solar Water Heater," Solar Energy, Vol.18, 1976, pp.327-335.

(2) Place, W., Daneshyar, M., and Kammerud, R., " Mean Monthly Performance of Passive Solar Water Heaters," in Proceedings of the 4th National Passive Solar Conference, Kansas City, MO, October 3-5, 1979, Vol. 4, pp.601-604 (Lawrence Berkeley Laboratory Report, LBL-9195).

(3) Bergquam, J.B., Young, M.F., Perry, S., and Baughn, J.W., "A Comparative Study of SDHW Systems in California," Report to the California Energy Commission, June 1979.

(4) Young, M.F. and Baughn, J.W., "Economics of Solar Domestic Hot Water Heaters in California," in Proceedings of Systems Simulation and Economic Analysis, San Diego, CA, January 23-25, 1980, pp.125-130.

(5) Farrington, R., Noreen, D., and Murphy, L.M., "A Comparative Analysis of Six Generic Solar Domestic Hot Water Systems," in Proceedings of System Simulation and Economic Analysis, San Diego, CA, January 23-25, 1980, pp.131-136.

(6) Fanney, A.H., Liu, S.T., and Hill, J.E., "Experimental Validation of Computer Programs for Solar Domestic Hot Water Systems," in Proceedings of the 3rd Annual Solar Heating and Cooling Research and Development Branch Contractors' Meeting,

Washington, D.C., September 24-27, 1978, pp.440-444.

(7) Fanney, A.H. and Liu, S.T., "Experimental System Performance and Comparison With Computer Predictions for Six Solar Domestic Hot Water Systems," in Proceedings of the International Solar Energy Society, Silver Jubilee Congress, Atlanta, Georgia, May 1979, Vol.2, pp.972-976.

(8) Fanney, A.H. and Liu, S.T., "Comparison of Experimental and Computer-Predicted Performance for Six Solar Domestic Hot Water Systems," ASHRAE Symposium on Solar Hot Water Systems, Los Angeles, CA, February 1980.

(9) Close, D.J., "The Performance of Solar Water Heaters With Natural Circulation," Solar Energy, Vol.6, 1962, pp.33-40.

(10) Bradley, J.M., "The Development of a Freeze-Tolerant Solar Water Heater Using Crosslinked Polyethylene as a Material of Construction," Report to Energy Research and Development Administration Division of Solar Energy, COO-2959-8, October 1977.

(11) Bradley, J.M., "The Development of a Freeze-Tolerant Solar Water Heater Using Crosslinked Polyethylene as a Material of Construction," presented at the 2nd Miami International Conference on Alternative Energy Sources, Miami Beach, FL, December 10-13, 1979.

(12) Mc Donald, T.W., Hwang, K.S., and DiCiccio, R., "Thermosiphon Loop Performance Characteristics: Part 1. Experimental Study," ASHRAE Transactions, Vol. 83, Part 2, 1977, pp. 250-259.

(13) Ali, A.F.M., and Mc Donald, T.W., "Thermosiphon Loop Performance Characteristics: Part 2. Simulation Program," ASHRAE Transactions, Vol. 83, Part 2, 1977, pp. 260-278.

(14) Mc Donald, T.W., and Ali, A.F.M., "Thermosiphon Loop Performance Characteristics: Part 3. Simulated Performance," ASHRAE Transactions, Vol. 83, Part 2, 1977, pp. 279-287.

(15) Mc Donald, T.W., Ali, A.F.M., and Sampath, S., "The Unidirectional Coil Loop Thermosiphon Heat Exchanger," ASHRAE Transactions, Vol. 84, Part 2, 1978, pp. 27-37.

(16) Mc Donald,T.W., and Sampath, S., "The Bidirectional Coil Loop Thermosiphon Heat Exchanger," ASHRAE Transactions, Vol. 86, Part 2, 1980, No. 2588, RP-188.

(17) American National Standard, "Solar Heat Exchangers," ANSI/ASME SES 1, May 1979 (Draft).

(18) Chinnappa, J.C.V. and Gnanalingam, K., "Performance at Colombo, Ceylon of a Pressurized Solar Water Heater of the Combined Collector and Storage Type," Solar Energy, Vol.15, 1973, pp.195-204.

(19) DeSa, V.G., "Solar-Energy Utilization at Dacca," Solar Energy, Vol.8, 1964, pp.83-90.

(20) Iqbal, M., "Free-Convection Effects Inside Tubes of Flat-Plate Solar Collectors," Solar Energy, Vol. 10, 1966, pp. 207-211.

(21) Gupta, C.L. and Garg, H.P., "System Design in Solar Water Heaters With Natural Circulation," Solar Energy, Vol. 12, 1968, pp. 163-182.

(22) Chinnery, D.N.W., "Solar Water Heating in South Africa," CSIR Research Report 248, 1971.

(23) Ong, K.S., "A Finite-Difference Method to Evaluate the Thermal Performance of a Solar Water Heater," Solar Energy, Vol.16, 1974, pp.137-147.

(24) Ong, K.S., "An Improved Computer Program for the Thermal Performance of a Solar Water Heater," Solar Energy, Vol.18, 1976, pp.183-191.

(25) Zvirin, Y., Shitzer, A., and Grossman, G., "The Natural Circulation Solar Heater-Models With Linear and Nonlinear Temperature Distributions," Int. J. Heat Mass Transfer, Vol.20, 1977, pp.997-999.

(26) Baughn, J.W. and Dougherty, D.A., "Experimental Investigation and Computer Modeling of a Solar Natural Circulation System," in Proceedings of the 1977 Annual Meeting of the American Section of the ISES, June 1977, Vol.1, pp.4.25-4.29.

(27) Baughn, J.W. and Dougherty, D.A., "Effect of Storage Height on the Performance of a Natural Circulation (Thermosyphon) Hot Water Systems," in Proceedings of the 2nd National Passive Solar Conference, Philadelphia, PA, March 16-18, 1978, Vol.2, pp.637-641.

(28) Dougherty, D.A. and Baughn, J.W., "Effects of Low Solar Input and Amount of Storage on Thermosyphon Hot Water System Performance," presented at the Winter Annual Meeting of the American Society of Mechanical Engineers, San Francisco, CA, December 10-15, 1978.

(29) Daneshyar, M., "Mean Monthly Performance of Solar Water Heaters With Natural Circulation," in Proceedings of the International Solar Energy Society, Silver Jubilee Congress, Atlanta, Georgia, May 1979, Vol.2, pp.983-987.

(30) Zvirin, Y., Shitzer, A., and Bartal-Bornstein, A., "On the Stability of the Natural Circulation Solar Heater," in Proceedings of the 6th International Heat Transfer Conference, Toronto, Canada, 1978, Vol.2, pp.141-145.

(31) Shitzer, A., Kalmanoviz, D., Zvirin, Y., and Grossman, G., " Experiments With a Flat Plate Solar Water Heating System in Thermosyphonic Flow," Solar Energy, Vol.22, 1979, pp. 27-35.

(32) Morrison, G.L., and Ranatunga, D.B.J., "Transient Response of Thermosyphon Solar Collectors," Solar Energy, Vol. 24, 1980, pp. 55-61.

(33) Morrison, G.L. and Ranatunga, D.B.J., "Thermosyphon Circulation in Solar Collectors," Solar Energy, Vol. 24, 1980, pp. 191-198.

(34) Jasinski, T. and Buckley, S., "Thermosyphon Analysis of a Thermic Diode Solar Heating System," presented at the Winter Annual Meeting of the American Society of Mechanical Engineers, Atlanta, Georgia, November 27-December 2,1977, ASME Paper No. 77-WA/Sol-9.

(35) Bernard, D., Durand, J., Zambrano, E., and Buckley, S., Transient Analysis of the Thermic Diode Solar Panel," in Proceedings of the 2nd National Passive Solar Conference, Philadelphia, PA, March 16-18, 1978, Vol.2, pp.469-473.

(36) Bernard, D.E. and Buckley, S., "Thermic Diode Performance Characteristics and Design Manual," in Proceedings of the International Soar Energy society, Silver Jubilee Congress, Atlanta, Georgia, May 1979. Vol. 2, pp. 1218-1222.

(37) Morris, W.S., "Natural Convection Solar Collectors," in Proceedings of the 2nd National Passive Solar Conference, Philadelphia, PA, March 16-18, 1978, Vol.2, pp.596-600.

(38) McClintock, M. and Frantz, M., "Solar Space Heat and Domestic Hot Water by a System Operating Both Actively and Passively," in Proceedings of the 2nd National Passive Solar Conference, Philadelphia, PA, March 16-18, 1978, Vol.2, pp.505-508.

(39) Bar-Cohen, A., "Thermal Optimization of Compact Solar Water Heaters," Solar Energy, Vol.20, 1977, pp.193-196.

(40) Close, D.J., "A Design approach for Solar Processes," Solar Energy, Vol. 11, 1967, pp. 112-122.

(41) Searcy, J.Q., "Hazardous Properties and Environmental Effects of Materials Used in Solar Heating and Cooling (SHAC) Technologies: Interim Handbook," prepared for U.S. Department of Energy, DOE/EV-0028, December 1978.

(42) Grossman, G., Shitzer, A., and Zvirin, Y., "Heat Transfer Analysis of a Flat-Plate Solar Energy Collector," Solar Energy, Vol.19, 1977, pp.493-502.

(43) Bliss, R.W., Jr., "The Derivations of Several Plate Efficiency Factors Useful in the Design of Flat-Plate Solar Heat Collectors," Solar Energy, Vol. 3, 1959, pp. 55-64.

(44) Liu, B.Y.H., and Jordan, R.C., "A Rational Procedure for Predicting the Long-Term Average Performance of Flat-Plate Solar-Energy Collectors," Solar Energy, Vol. 7, 1963, pp. 53-74.

(45) Klein, S.A., Duffie, J.A., and Beckman, W.A., "Transient Considerations of Flat-Plate Solar Collectors," ASME J. Engineering for Power, April 1974, pp. 109-113.

(46) Keller, J.B., "Periodic Oscillations in a Model of Thermal Convection," J. Fluid Mechanics, Vol. 26, 1966, pp. 599-606.

(47) Wissler, E.H., Isbin, H.S., and Amundson, N.R., "Oscillatory Behavior of a Two-Phase Natural-Circulation Loop," A.I.Ch.E. Journal, Vol. 2, 1956. pp. 157-162.

(48) Welander, P., "On the Oscillatory Instability of a Differentially Heated Fluid Loop," J. Fluid Mechanics, Vol. 29, 1967, pp. 17-30.

(49) Creveling, H.F., DePaz, J.F., Baladi, J.Y., and Schoenhals, R.J., "Stability Characteristics of a Single-Phase Free Convection Loop," J. Fluid Mechanics, Vol.67, 1975, pp.65-84.

(50) Greif, R., Zvirin, Y., and Mertol, A., "The Transient and Stability Behavior of a Natural Convection Loop," J. Heat Transfer, Vol.101, 1979, pp.684-688.

(51) Mertol, A., "Heat Transfer and Fluid Flow in Thermosyphons," Ph. D. Dissertation, University of California, Berkeley, May 1980.

(52) Mertol, A., Greif, R., and Zvirin, Y., "The Transient, Steady-State and Stability Behavior of a Thermosyphon with Throughflow," Int. J. Heat Mass Transfer, Vol.24, 1981, pp.

621-633.

(53) Zvirin, Y., Jeuck III, P.R., Sullivan, C.S., and Duffey, R.B., "Experimental and Analytical Investigation of a PWR Natural Circulation Loop," ANS/ENS Thermal Reactor Safety Meeting, Knoxville, TN, April 1980.

(54) Berdahl, P., Grether, D., Martin, M., and Wahlig, M., "California Solar Data Manual," Report to the California Energy Commission, March 1978.

(55) Huang, B.J., "Similarity Theory of Solar Water Heater with Natural Circulation," Solar Energy, Vol. 25, 1980, pp. 105-116.

(56) Mertol, A., Place, W., Webster, T., and Greif, R., "Thermosiphon Water Heaters with Heat Exchangers," in Proceedings of the AS/ISES Conference, Phoenix, Arizona, June 2-6, 1980, Vol. 3.1, pp. 309-313 (Lawrence Berkeley Laboratory Report, LBL-10033, 1980).

(57) Houston Chemical Company, Division of PPG Industries Inc., "Solar Heat Transport Fluids for Solar Energy Collection Systems (A Collection of Quarterly Reports)", Report No. DOE/NASA CR-150560, January, 1978.

(58) Moses, P.J., "Private Communications", Dow Chemical Company, Engineered Products T.S. and D. Larkin Laboratory, Midland, Michigan.

APPENDIX

SUMMARIES OF VARIOUS THERMOSIPHON PUBLICATIONS

- For a specific thermosiphon configuration, Close [9] observed experimentally that the average collector temperature was only slightly higher than the average tank temperature. Based on this experimental fact, he developed a simple analytic model for predicting the daytime performance of such a thermosiphon under the conditions of no draw and clear sunshine. Using a simple heat balance for the entire thermosiphon system, he was able to generate a differential equation describing the time variation of the average tank temperature. The solution to the differential equation is an analytic function under the condition of a sinusoidal time variation of the ambient air temperature and the solar irradiance. The method is very simple and quite accurate in predicting the performance of the specific system configuration under the specific environmental condition considered. The method is limited by its empirical foundation which does not provide information about variations in system performance as a function of changes in system parameters or environmental conditions.

- Chinnapa and Gnanalingam [18] described an alternate scheme for including the solar radiation data by using cumulative partial sums each hour.

- De Sa [19] generated a lumped parameter heat balance equation which he solved numerically using actual solar radiation data and a half-hour time step. The model was used to predict the tank temperature as a function of time for a day with no hot water draw. Experimental results presented agreed with predictions within about 1.1°C (2°F).

- Iqbal [20] performed experimental and theoretical studies of the effects of free convection superimposed on forced flow in uniformly heated inclined tubes. The studies identified the tube tilt angle for transferring heat from the absorber plate to the circulating fluid. Total system performance was not optimized as a function of tilt angle.

- Gupta and Garg [21] improved on the Close analysis by incorporating a collector plate efficiency factor and approximating the variable ambient conditions by using Fourier series expansions for the ambient temperature and the solar irradiance. They also made daytime and nighttime experimental observations. The theory and experiment agreed well during the daytime hours; the observed nighttime system loss rate was almost halfway between the loss rates predicted for the two extreme cases of perfect coupling high reverse flow and perfect decoupling no reverse flow between the collector and storage tank.

- Chinnery [22] investigated experimentally the effect of collector characteristics, tank elevation, and climate on collection efficiency. He experimentally determined the loss of pressure in the absorbers as a function of flow rate and the results, which were given in graphical form, were used in calculating maximum pipe

lengths in the primary flow circuit. He also developed a mathematical formulation which explained how reverse flow could occur under certain specific conditions but he made no predictions of the magnitude of the effect on system performance.

- Ong [23] extended the Close analysis by using a finite difference solution procedure and a different formulation of the plate efficiency factor. He retained the assumption that the mean temperature of the absorber unit and the storage tank are equal, but the plate and fin efficiency, plate heat-loss coefficient, tube-water film heat-transfer coefficient, friction factor and physical properties of the water were allowed to vary with temperature and water flow rate, evaluating each of these variables according to the flow and temperature conditions at the instant of time considered. In a later paper Ong [24] improved the analysis by dividing the convective loop into several sections on each of which an energy balance was performed. In both studies, Ong predicted and measured the mass flow rate, mean tank temperature, collector efficiency and mean system efficiency. The experimental value for mean system efficiency was larger than the prediction of the simple model by about of a factor of 1.25. The improved analysis reduced the error to less than half.

- Zvirin, Shitzer and Grossman [25] developed a mathematical model for obtaining the steady-state temperature distribution and flow rate in thermosiphons.

- Baughn and Daugherty [26-28] both analytically and experimentally investigated the daytime behavior of a thermosiphon water heater as a function of collector area, storage tank elevation, and solar irradiance.

- Daneshyar [29] used a variation of the Close analysis to predict average monthly system performance assuming a batch draw at the end of the day and no night losses. A significant feature of Daneshyar's analysis was the prediction of available solar radiation based on easily accessible meteorological data. He also conducted experiments which indicated that his theoretical predictions of system performance were within about 10% of the observed performance.

- Zvirin, Shitzer and Bartal-Bornstein [30] developed an analytic one-dimensional model for the thermosiphon loop. Stability of a steady-state motion in the system was analyzed by using the linearized stability equations and computing the resulting eigenvalues. They found perturbation modes which decay very slowly and oscillatory modes with period on the order of the time required to circulate the loop. They also predicted system instability during periods of high draw rates.

- Shitzer, Kalmanoviz, Zvirin and Grossman [31] studied the daytime behavior of thermosiphon using thermocouples and a special low-resistance flow meter based on thermal dissipation tracing. The results showed essentially linear temperature distributions in both the collector and the tank, for the no-draw situation. Water flow

rate was found to be about 33% lower than the rate predicted theoretically by the authors. Daytime fluctuations in the water flow rate were observed, but the authors were unclear whether the effect was real or an artifact of the instrumentation. Similar flow fluctuations have been predicted for a non-solar convective loop by Keller [46]. Furthermore, flow oscillations have also been predicted theoretically or observed experimentally in non-solar convection loops by Wissler, Isbin and Amundson [47], Welander [48], Creveling, De Paz, Baladi and Schoenhals [49], Greif, Zvirin and Mertol [50], Mertol [51], Mertol, Greif and Zvirin [52], and Zvirin, Jeuck III, Sullivan and Duffey [53].

- Morrison and Ranatunga [32,33] measured thermosiphon flow rates using a laser doppler anemometer and developed an analytic model for describing the transient flow process. Their studies included an investigation of system response to step changes in the solar radiation. Their results showed that, although there are long time delays associated with the development of the thermosiphon flow, the energy collection capability is not significantly affected by flow delays.

- Mc Donald, Hwang and DiCiccio [12], Ali and Mc Donald [13] and Mc Donald and Ali [14] studied the performance of a two-phase thermosiphon waste heat recovery system. Their results indicated that optimum performance may be expected from a thermosiphon loop when the evaporator and condenser tubes are oriented in such a way that the condenser is nowhere flooded, no dryout occurs in the evaporator, and negligible liquid is carried over from the evaporator into the condenser. Mc Donald, Ali and Sampath [15] and Mc Donald and Sampath [16] investigated both bi-directional and uni-directional two-phase coil loop thermosiphon heat exchangers both experimentally and by computer simulation. Their results showed that single tube two-phase thermosiphon loops may be designed to provide peak performance over a modest range of operating temperature differences. Uni-directional loops offer a higher performance than bi-directional loops but are more sensitive to changes in the imposed temperature differences.

- Huang [55] studied common thermosiphon solar water heater systems, without a heat exchanger in the storage tank, by solving a dimensionless form of the energy, momentum and continuity equations using a finite difference technique. This is essentially the same technique used in the present work except for differences in several important assumptions: Both studies assumed one dimensional velocity and temperature distributions in the system, negligible heat capacity of system construction materials, negligible axial conduction and a sinusoidal solar input. Huang [55], however, did not consider transient heat transfer inside and heat loss from connecting pipes and storage tank, and considered only laminar flow in the system. In addition, a parallel plate collector, constant ambient temperature, and no draw were assumed. The DLM on the other hand considered transient heat transfer in connecting pipes, heat loss from all components, turbulent and laminar flows, parallel tube collector, draw profile, as well as nighttime reverse flow. Huang [55]

performed a parametric analysis for ten different system parameters that showed the effect on flow rate and mean daily efficiency of tank volume, solar insolation, tank height and system flow resistance. These results indicated that the system performance was essentially independent of tank height for low flow resistance systems but increased with height for high resistance systems.

ACKNOWLEDGEMENT

This work was supported by the Research and Development Branch, Passive and Hybrid Division of the Office of Solar Applications for Buildings of the U.S. Department of Energy under Contract No. W-7405-ENG-48.